Molecular and genetic regulation of pig pancreatic islet cell development
— **Source link** ⧉

Seokho Kim, Robert L. Whitener, Heshan Peiris, Xueying Gu ...+11 more authors

Institutions: Stanford University, University of California, Davis, University of California, Irvine, Allegheny Health Network

Related papers:

- Molecular and genetic regulation of pig pancreatic islet cell development.

- Gene expression profiling of a mouse model of pancreatic islet dysmorphogenesis

- Gene Signature of the Human Pancreatic ε Cell.

- Pancreas patch-seq links physiologic dysfunction in diabetes to single-cell transcriptomic phenotypes

- Patterns of differential gene expression in a cellular model of human islet development, and relationship to type 2 diabetes predisposition

Share this paper: 𝐟 🐦 in ✉

View more about this paper here: https://typeset.io/papers/molecular-and-genetic-regulation-of-pig-pancreatic-islet-36cn8qn6ik

1   **Molecular and genetic regulation of pig pancreatic islet cell development**

2

3

4   Seokho Kim[1,9], Robert L. Whitener[1,9], Heshan Peiris[1], Xueying Gu[1], Charles A. Chang[1],

5   Jonathan Y. Lam[1], Joan Camunas-Soler[2], Insung Park[3], Romina J. Bevacqua[1], Krissie Tellez[1],

6   Stephen R. Quake[2,4], Jonathan R. T. Lakey[5], Rita Bottino[6], Pablo J. Ross[3], Seung K. Kim[1,7,8]

7

8   [1]Department of Developmental Biology, Stanford University School of Medicine,

9   Stanford, CA, 94305 USA

10   [2]Department of Bioengineering, Stanford University, Stanford, CA, 94305 USA

11   [3]Department of Animal Science, University of California Davis, Davis, CA, 95616 USA

12   [4]Chan Zuckerberg Biohub, San Francisco, CA 94518, USA.

13   [5]Department of Surgery, University of California at Irvine, Irvine, CA, 92868 USA

14   [6]Institute of Cellular Therapeutics, Allegheny Health Network, Pittsburgh, PA, 15212 USA

15   [7]Department of Medicine, Stanford University School of Medicine, Stanford, CA, 94305 USA

16   [8]Stanford Diabetes Research Center, Stanford University School of Medicine,

17   Stanford, CA, 94305 USA

18

19   [9]These authors contributed equally

20

21   Correspondence and requests for materials should be addressed to S.K.K (email:

22   seungkim@stanford.edu)

23

24   **Key Words: pancreas; metabolism; organogenesis; β-cell; α-cell; δ-cell; diabetes mellitus**

25

26   **Summary Statement:** This study reveals transcriptional, signaling and cellular programs

27   governing pig pancreatic islet development, including striking similarities to human islet

28   ontogeny, providing a novel resource for advancing human islet replacement strategies.

29 **Abstract**

30   Reliance on rodents for understanding pancreatic genetics, development and islet function
31   could limit progress in developing interventions for human diseases like diabetes mellitus.
32   Similarities of pancreas morphology and function suggest that porcine and human pancreas
33   developmental biology may have useful homologies. However, little is known about pig
34   pancreas development. To fill this knowledge gap, we investigated fetal and neonatal pig
35   pancreas at multiple, crucial developmental stages using modern experimental approaches.
36   Purification of islet β-, α- and δ-cells followed by transcriptome analysis (RNA-Seq) and
37   immunohistology identified cell- and stage-specific regulation, and revealed that pig and human
38   islet cells share characteristic features not observed in mice. Morphometric analysis also
39   revealed endocrine cell allocation and architectural similarities between pig and human islets.
40   Our analysis unveiled scores of signaling pathways linked to native islet β-cell functional
41   maturation, including evidence of fetal α-cell GLP-1 production and signaling to β-cells. Thus,
42   the findings and resources detailed here show how pig pancreatic islet studies complement
43   other systems for understanding the developmental programs that generate functional islet cells,
44   and that are relevant to human pancreatic diseases.
45

Introduction

Progress from studies of pancreas biology in humans (Hart and Powers, 2019; Hrvatin et al., 2014b) has advanced our understanding of post-natal islet regulation and function. The recognition that mouse pancreas biology – while essential – has limitations for understanding human pancreas formation or diseases (Hattersley and Patel, 2017; Maestro et al., 2007), has intensified interest in experimental systems that more closely reflect human pancreas development (McKnight et al., 2010; Pan and Brissova, 2014). There is a specific, crucial knowledge gap in our understanding of human islet and pancreas development from mid-gestation through neonatal and juvenile stages, a period when critical aspects of islet development are known to occur (Arda et al., 2016). The use of human primary tissues to address such questions is limited by inter-individual heterogeneity, unpredictable and restricted access to tissue from key developmental stages, and challenges implementing high-throughput molecular approaches. Likewise, reconstitution of islet development from stem cell sources or fetal human cell lines remains imperfect (Sneddon et al., 2018), thereby limiting interpretation of developmental studies in those systems.

Humans and pigs are omnivorous mammals with similar physiology and metabolic diseases, including diabetes mellitus and its complications, from diet-induced obesity, insulinopathy and β-cell stress (Dyson et al., 2006; Lim et al., 2018; Renner et al., 2013). Recent experimental advances expand possible studies of pig pancreas development to include gain- and loss-of-function genetics (Kemter et al., 2017; Matsunari et al., 2013; Sheets et al., 2018; Wu et al., 2017), fetal surgery and immunomodulation (Fisher et al., 2013), and primary islet cell genetics (Peiris et al., 2018). Prior studies of pig pancreas development have largely relied on immunohistological survey of tissue cell types (Carlsson et al., 2010; Ferrer et al., 2008; Hassouna et al., 2018; Nagaya et al., 2019). Moreover, studies linking hallmark islet functions, like regulated insulin secretion and dynamic changes in gene expression at advancing developmental stages, have not been previously reported (Mueller et al., 2013). Thus, pancreas and metabolic research could benefit from systematic application of powerful methods like cell purification by flow cytometry, high-throughput transcriptome analysis, and islet physiological studies across a comprehensive range of pig developmental stages.

Here we apply these and other modern approaches to delineate pig pancreas development, with a focus on islet β-cells, the sole source of insulin, and α-cells, the principal systemic source of the hormone glucagon. Dysregulation of hormone secretion by these cells is thought to be a leading cause of both type 1 diabetes (T1D) and type 2 diabetes (T2D) in humans (Holst et al., 2017; Lee et al., 2016). Our findings provide evidence of greater similarity between pig and

80   human β-cells and α-cells than to cognate mouse cells, and demonstrate how studies of pig

81   pancreatic cells can advance our understanding of the genetic, molecular, signaling and

82   physiological programs that generate functional pancreatic islet cells.

83

84   **Results**

85   **Pancreas dissociation and FACS purification of islet cells from fetal and neonatal pigs**

86   To measure gene expression and functional changes in the developing pig pancreas, we

87   established a reliable infrastructure to procure pancreata from fetal or neonatal pigs using

88   rigorous criteria that optimized tissue quality and gene expression analysis (Fig. 1A). To

89   investigate the crucial period of ontogeny culminating in functional islet cells, we systematically

90   isolated pancreata from gestational days (d) 40, 70, 90 and post-natal days (P) 8 and 22 (Fig.

91   1A). We surveyed sorting methods based on cell surface epitopes, like in prior work with mouse

92   and human cells (Arda et al., 2016; Arda et al., 2018; Sugiyama et al., 2013), but have not yet

93   achieved reliable cell fractionation based with this strategy (R. Whitener and S. K. Kim, unpubl.

94   results). Instead, we used intracellular sorting with specific antibodies against insulin-, glucagon-

95   and somatostatin- to isolate β-, α- and δ-cells, respectively, from fetal or neonatal pancreata

96   (Fig. S1A), like in prior work on human islets (Arda et al., 2016; Hrvatin et al., 2014a; Peiris et

97   al., 2018). Quantitative RT-PCR (qRT-PCR: Fig. 1B) confirmed enrichment or depletion of

98   expected marker genes for β- (*INS*), α- (*GCG*), δ- (*SST*), ductal (*KRT19*) and acinar cells

99   (*AMY2*).

100   To obtain comprehensive gene expression profiles, we performed RNA-Seq on 37 libraries

101   generated from fetal and neonatal pancreatic cells (Table S1). An average of 7 million reads per

102   sample library uniquely mapped to a current pig reference transcriptome (Sscrofa11.1).

103   Unsupervised hierarchical clustering of transcriptome data with Pearson correlation analysis

104   revealed distinct expression profiles that changed with advancing developmental stage within

105   specific cell types (Fig. S1B). Principal component analysis with these samples showed that

106   transcriptomes clustered in the first principal component according to cell type (β-, α- or δ-cells:

107   PC1, 35% of variance), and according to advancing developmental stage in the second principal

108   component (PC2, 25% of variance: Fig. S1C). Samples from 'late fetal' stages d70 and d90

109   clustered closely and separately from d40 samples, and were grouped together for subsequent

110   analysis (pig development *in utero* averages 114 days). In summary, our cell purification

111   strategy generated high-quality gene expression profiles of developing pig β-, α- and δ-cells.

112

113   **High-depth transcriptome maps in pig β-, α- and δ-cells.**

114   To evaluate stage-specific differential gene expression, we analyzed transcriptome data in
115   early fetal (d40), late fetal (d70 and d90) and neonatal stages (P8-P22) (Fig. 1C-H). We used
116   the DESeq2 algorithm (Love et al., 2014) to find differentially expressed genes (DEGs)
117   encoding transcripts whose level changed at least 1.5-fold (adjusted *P*<0.05) between these
118   stages in β-, α- or δ-cells. Between early and late fetal stages, we identified 2696 DEGs in β-
119   cells, with transcripts from 1270 genes increased and 1426 decreased. Between late fetal and
120   neonatal stages, we identified 1463 DEGs: transcripts from 785 genes increased, and 678
121   genes decreased (Fig. 1C and Table S2). In α-cells between early and late fetal stages, we
122   identified 2823 DEGs with transcripts from 1311 genes increased and 1512 genes decreased.
123   Between late fetal and neonatal stages, we identified 2291 DEGs: transcripts from 1200 genes
124   increased, and 1091 genes decreased (Fig. 1E and Table S2). In δ-cells between late fetal and
125   neonatal stages, we identified 1698 DEGs with transcripts from 985 genes increased, and 713
126   genes decreased (Fig. 1G and Table S2). Among DEGs, we observed subsets of genes
127   enriched in either fetal or neonatal stages in β-, α- or δ-cells, confirming the presence of
128   regulated developmental gene expression programs in specific pig islet cell types. Transcript
129   abundance data from β-, α- and δ-cells are also provided in a searchable dataset (Table S3).

130   To evaluate coherent patterns of differential gene expression, and effects on signaling
131   pathways at specific stages, we performed gene ontology (GO) term analysis for biological
132   processes with Clusterprofiler (Yu et al., 2012). In the transition from the early to the late fetal
133   stages, we observed enrichment of specific terms linked to islet β- or α-cell development, like
134   glucose homeostasis, endocrine pancreas development, store-operated calcium entry,
135   response to glucose, and regulation of hormone secretion (Fig. 1D,F). In the transition from late
136   fetal and neonatal stages in β-, α- or δ-cells, we observed enrichment of biological processes
137   distinct from those at earlier developmental stages. These included MAP kinase signaling,
138   hormone secretion, cAMP metabolic process, and Rho protein signaling transduction (Fig.
139   1D,F,H).

140

141   **Cell type- and stage-specific gene expression in pig islet β-, α- and δ-cells**

142   Next, we assessed expression of genes thought to regulate development of β-, α- and δ-cells
143   (Fig. 2A-H). Since transcription factors, including PDX1, NKX6.1 and ARX, are known to govern
144   β- and α-cell differentiation in mouse and human islet cells (Aguayo-Mazzucato et al., 2011;
145   Artner et al., 2007; Artner et al., 2010; Collombat et al., 2003; Schaffer et al., 2013), we
146   assessed expression of transcription factors in pigs. Transcripts encoding the factors PDX1,

147   MAFA and NKX6.1 were highly enriched in pig β-cells throughout development, while genes

148   encoding ARX and IRX2 were exclusively expressed in pig α-cells (Fig. 2A, B). Unlike in mice,

149   MAFB is known to be expressed in both human β- and α-cells (Arda et al., 2016; Blodgett et al.,

150   2015). Notably, we observed that *MAFB* was expressed in both pig β- and α-cells (Fig. 2A). As

151   expected, pig δ-cells expressed genes encoding transcription factors such as *HHEX*, *PDX1*, and

152   the transporter *RBP4*, consistent with previous findings in other systems (Muraro et al., 2016)

153   (Fig. 2A,C). GLP1R is known to be highly expressed in human β-cells and involved in β-cell

154   function (Dai et al., 2017). Similar to human, *GLP1R* mRNA was highly expressed in pig β-cells

155   (Fig. 2D). Urocortin3 (UCN3) secreted by β-cells binds to corticotropin-releasing hormone

156   receptor 2 (CRHR2) in δ-cells, stimulating somatostatin secretion (van der Meulen et al., 2015).

157   In accordance with these previous findings, we observed that *UCN3* and *CRHR2* mRNA are

158   highly expressed in pig β-cells and δ-cells, respectively, raising the possibility that this signaling

159   axis is conserved in the pig (Fig. 2D).

160   We also observed dynamic expression of genes regulating islet cell proliferation and function

161   in developing pig β- and α-cells (Fig. 2E-H). For example, *MKI67*, *BUB1B* and *NUSAP1*, which

162   encode products known to regulate mitosis and cell cycle progression, declined as β- and α-cell

163   development advanced (Fig. 2E). To validate these findings, we used immunohistology to

164   quantify the nuclear factor Ki67, a marker of cell proliferation encoded by *MKI67* in multiple

165   species, including pigs, humans and mice (Arda et al., 2016; Georgia and Bhushan, 2004; Meier

166   et al., 2008; Teta et al., 2007). In pigs, pancreas immunostaining revealed a high percentage

167   (10%) of Ki67^{+} early fetal islet cells (d40), that declined to 2% by late fetal and neonatal stages,

168   then further declined to <0.1% by adulthood (Fig. 2F and Fig. S2). These changes were

169   mirrored by mRNA levels encoding *MKI67* (Fig. 2E). Thus, we observed evidence of vigorous

170   fetal-stage proliferation of islet cells that, like in mice and humans, declined further after birth.

171   Likewise, we found that expression of 'disallowed' genes like *COX5A, SLC16A1*, *MGST3*

172   and *LDHA*, originally identified in β-cells and thought to restrain β-cell function and maturation

173   (Lemaire et al., 2016; Pullen et al., 2017; Pullen et al., 2010; Sekine et al., 1994), declined

174   during development (Fig. 2G). We also detected dynamic or cell type-specific expression of

175   genes encoding established effectors of islet hormone secretion, like the proprotein convertase

176   *PCSK2*, the ion transporter *SLC30A8*, and the glucose transporter *SLC2A2* (Fig. 2H). These

177   data delineate gene expression changes at genome-scale that orchestrate age-dependent

178   changes in proliferation and maturation of islet β-, α- and δ-cells. Thus, our studies revealed

179   both similarities of (1) *cell type-specific* gene expression between pig and human islet β-, α- and

180   δ-cells, and (2) conserved *stage-specific* gene expression dynamics in pigs.

181

Stage-specific islet cell allocation and production of transcription factors

183   To verify further our RNA-Seq findings in developing islets, we performed immunostaining of

184   pig pancreata at specific developmental stages. At fetal stages, islet β-, α- and δ-cells formed

185   small clusters, which enlarged subsequently in neonatal and adult pancreas (Fig. 3A-C and Fig.

186   S3A). Thus, like in other species (Carlsson et al., 2010; Jeon et al., 2009; Jorgensen et al.,

187   2007), islet cells formed clusters at the inception of their ontogeny, then continued their

188   morphogenesis in multicellular structures through post-natal stages. In fetal, neonatal and adult

189   islets, standard morphometry revealed that differentiation of islet cells into specific lineages was

190   dynamic (Fig. S3A,B). In early fetal pancreas, the number of α-cells is slightly higher than that of

191   β-cells, while the δ-cell fraction was very low (<4%). However, from late fetal to neonatal stages,

192   the number of β-cells is higher than that of α-cells, while the number of δ-cells is similar to that

193   of α-cells (Fig. S3B). Consistent with our RNA-Seq data, antibodies that detect the transcription

194   factors (TFs) PDX1, NKX6.1 and MAFB showed restricted production in specific islet cell

195   subsets. In β-cells, we detected nuclear PDX1, NKX6.1. By contrast, we detected MAFB protein

196   in both β- and α-cells (Fig. 3D-F). Unlike in mice, human β-cells express the transcription factors

197   SIX3 and SIX2 in an age-dependent manner; moreover human α-cells do not express *SIX3* or

198   *SIX2* (Arda et al., 2016). Immunohistology (Fig. 3G) demonstrated SIX3 production specifically

199   in a subset of adult β-cells, and qRT-PCR (Fig. 3H) of pig islets revealed adult-specific

200   production of SIX3. We observed a similar age-dependent expression of *SIX2* (Fig. 3I); the

201   absence of antibodies for pig SIX2 precluded immunohistology studies. In summary, stage-

202   specific and cell-specific expression of multiple TFs in pig islets resembled that observed

203   previously in human islet cell subsets.

204

Similarities of pig and human β-cells and α-cells

206   Beyond assessment of TFs, we sought independent evidence of similarities between pig,

207   human and mouse β-cells. We used unsupervised hierarchical clustering with distance matrix

208   analysis of our RNA-Seq data, and extant human and mouse islet cell bulk RNA-Seq data (Arda

209   et al., 2016; Blodgett et al., 2015; Qiu et al., 2017). This analysis suggested that neonatal β-cell

210   transcriptomes in pig and human were globally more similar than to the β-cell transcriptome of

211   mice (Fig. 4A). The absence of sufficient fetal or neonatal mouse α- or δ-cell transcriptome data

212   precluded analogous global comparisons of human, pig and mouse α-cells or δ-cells. GO term

213   enrichment analysis also revealed differential molecular signatures between neonatal pig and

214   juvenile human β-cells. Significantly enriched pig pathways were associated with proliferation,

215   while pathways enriched in human juvenile islet β-cells included those regulating β-cell

216   secretory function (Fig S4 and Table S5). This is consistent with prior observations, including

217   relatively higher proliferation in neonatal pig β-cells compared to juvenile human β-cells (Arda et

218   al., 2016).

219   Next, we performed pairwise comparison of pig and human (Blodgett et al., 2015) cells from

220   fetal and postnatal stages (Fig. 4B-G and Table S4). This analysis revealed conserved cell type-

221   specific and stage-specific regulation of multiple factors. For example, *GLP1R* encodes a G

222   protein-coupled receptor for the incretin hormone GLP-1. Like in humans (Dai et al., 2017),

223   *GLP1R* is expressed in pig β-cells but not α-cells and this expression increases from fetal to

224   neonatal stages (Fig. 4B). By contrast the G protein coupled receptor encoded by *GPR87* is

225   expressed in pig and human α-cells but not β-cells and has increasing expression during

226   postnatal islet maturation (Fig. 4C). Similarities in cell type-specificity or stage-specific

227   expression for other regulators, including *DNMT1*, *PPID*, *KLF9*, and *DCHS1,* provide further

228   evidence of conserved genetic programs underlying pig and human β- and α-cell development

229   (Fig. 4D-G). Taken together, our analysis of specific islet TF's, global gene expression

230   similarities in β-cells, similarities of developmental islet cell allocation, and of islet morphology

231   provide evidence of remarkable similarities in pig and human β-cell development.

232

233   **Dynamic gene regulation during pig β- and α-cell development**

234   Our studies of pig islet development provided an unprecedented opportunity to assess gene

235   expression dynamics throughout fetal and postnatal stages. From the early fetal to neonatal

236   stage, we identified 3,111 genes in β-cells and 3,668 genes in α-cells with dynamic expression

237   (Fig. 5A,B and Table S6). Thus, our analysis permitted grouping of genes in 'clusters', based on

238   the sequence of changes observed between three discrete developmental periods. For example,

239   we observed genes in β- and α-cells that increased through late fetal stages, then did not

240   change thereafter (cluster 2, 'Up_NC') and other genes whose transcript levels declined through

241   late fetal stages then did not change thereafter (cluster 7, 'Down_NC') (Table S6). We grouped

242   genes in 8 clusters (Up_Down, Down_Up, etc.), and GO term analysis of each cluster revealed

243   dynamic biological processes (Fig. 5A,B and Fig. S5A,B). For example, we observed that the β-

244 and α-cell "Down_NC" clusters were significantly enriched for genes that regulate cell
245 proliferation and cell cycle progression (like *CDK2, CDK14* and *CDC20*; Fig. 5A,B and Table
246 S6). The "Up_NC" cluster in both cell types was enriched for genes associated with multiple
247 signaling pathways involved in glucose and steroid hormone signaling (Fig. S5A,B). Thus, the
248 data identified multiple biological processes involved in islet differentiation and maturation that
249 are dynamically regulated in development.

250   The frequency of transcript measurement in our workflow also identified unanticipated gene
251 expression dynamics in developing β- and α-cells, particularly in gene clusters with "Up_Down"
252 or "Down_Up" trajectories (clusters 3 and 6: Fig. 5C,D). For example, from fetal to neonatal
253 stages in islet β-cells, we observed increased levels of transcript encoding pyruvate
254 dehydrogenase kinase 4 (PDK4), a factor previously characterized (Pullen et al., 2017) as
255 'disallowed' in β-cells (Fig. 5C). Consistent with this, we observed that expression of
256 *PPARGC1A*, a known positive regulator of *PDK4* transcription (Wende et al., 2005) also
257 increased at this stage in β-cell development ("NC_Up" cluster; Table S6). Thus, unlike other
258 disallowed genes whose expression continuously declined in developing β- and α-cells, *PDK4*
259 expression appeared to increase after late fetal stages, raising the possibility of as-yet
260 unidentified functions for PDK4 in pig β-cell development.

261   In human diabetes, genetic risk may reflect monogenic or polygenic mechanisms
262 (Cerolsaletti et al., 2019; Hattersley and Patel, 2017; Pearson, 2019; Sanyoura et al., 2018). We
263 hypothesized that causal genes in monogenic forms of diabetes including neonatal diabetes
264 mellitus (NDM) and maturity onset diabetes of the young (MODY) might be developmentally
265 regulated. Thus, we compared expression dynamics of 33 genes, linked by prior studies to
266 human NDM and MODY (Velayos et al., 2017; Yang and Chan, 2016), and with known pig
267 orthologues (Table S7). We found ten genes dynamically expressed between fetal and neonatal
268 stages in pig β-cells. Of those, six genes - *INS, STAT3, NEUROG3, GATA4, SLC2A2*, and
269 *PCBD1* - are known to have dynamic expression in human β-cells. In pig α-cells, 13 causal
270 genes are dynamically expressed, with four - *WFS1, NEUROG3, CEL*, and *GATA6* - known to
271 have changing expression in human α-cells. We also identified seven genes which are
272 differentially expressed between the late fetal and neonatal stages in pig δ-cells. Thus our work
273 reveals pig orthologues of causal genes for MODY and NDM whose expression changes in
274 development of multiple islet cell types, identifying opportunities for investigating native dynamic
275 regulation of these genes.

9

276   *PCSK1* encodes an endopeptidase normally expressed in intestinal L-cells to regulate GLP-1

277   production (Rouille et al., 1995; Steiner, 1998), and in β-cells for proinsulin processing.

278   Unexpectedly, we observed a transient increase of *PCSK1* mRNA in fetal α-cells (Fig. 5E);

279   immunostaining confirmed that PCSK1 protein was produced in a subset of late fetal d70 α-cells

280   but not in early fetal or adult α-cells (Fig. 5F). Consistent with these findings, ELISA

281   quantification of bioactive GLP-1 revealed abundant production in d70 islets that decreased

282   thereafter and was undetectable in adult islets (Fig. 5G). Likewise, *DPP4* encodes a protease

283   that inactivates GLP-1 and whose expression is extinguished in postnatal human β-cells (Arda

284   et al., 2016; Blodgett et al., 2015). However, we observed a significant *increase* of *DPP4* mRNA

285   and protein levels in β-cells at late fetal stages, when β-cells also express *GLP1R* (Fig. 5H,I and

286   Table S3). Together, these findings provide evidence that fetal α-cells transiently produce GLP-

287   1, and that GLP-1/GLP1R/DPP4 signaling interactions could regulate fetal β-cell development.

288

289   **Genetic regulation of β-cell functional maturation**

290   Age-dependent enhancement of glucose-regulated insulin secretion has been described in

291   rodents and humans (Aguayo-Mazzucato et al., 2011; Arda et al., 2016; Avrahami et al., 2015;

292   Blum et al., 2012; Rorsman et al., 1989). In pigs, prior studies of islet insulin secretion have

293   focused on postnatal stages (Mueller et al., 2013), but did not compare fetal to neonatal stages.

294   We compared glucose-stimulated insulin secretion in islets isolated from late fetal (d70) or

295   weaning-age donors (P22). Glucose or IBMX, a potentiator of intracellular cAMP levels and

296   insulin secretion, did not significantly increase insulin output by fetal islets in static batch

297   cultures (Fig. 6A). Moreover, insulin secretion by fetal islets in the 'basal' 2.8 mM glucose

298   condition was higher than that observed from P22 islets (Fig. 6A). In P22 pig islets, glucose or

299   glucose + IBMX significantly increased insulin secretion (Fig. 6A), though to a lesser degree

300   than in human juvenile islets (Arda et al 2016). The pattern of declining basal secretion

301   accompanied by enhanced glucose-regulated insulin secretion in pig islets is similar to findings

302   from prior studies of isolated late-fetal and neonatal rodent islets (Sodoyez-Goffaux et al., 1979),

303   and provides evidence of post-natal pig β-cell functional maturation.

304   To assess the genetic basis of this maturation, we compared transcriptomes from late fetal

305   and P22 β-cells (Fig. 6B). DESeq2 analysis revealed significantly increased expression of 924

306   genes and decreased expression of 895 genes between late fetal (both E70 and E90) and P22

307   (Table S8). GO term analysis revealed that up-regulated transcripts were encoded by genes

308   associated with pathways involved in insulin secretion (Fig. 6C and Table S9). Intracellular

10

309   cAMP and Ca^{2+} levels are crucial regulators of insulin exocytosis (Tengholm and Gylfe, 2017).

310   We observed that transcripts of genes encoding channels activated by cAMP, such as HCN4

311   and KCNQ1 were up-regulated (Fig. 6D). We also found increased expression of genes

312   regulating cytoplasmic Ca^{2+} concentration or genes involved in Ca^{2+}-mediated signaling

313   pathways such as CRACR2A and CAMK2D (Fig. 6D). Phosphodiesterases (PDEs), which

314   induce hydrolysis of cAMP to 5'-AMP, were also up-regulated by stage P22 (Fig. 6C). These

315   findings are consistent with the view that cAMP signaling 'tone' may be relatively high in fetal

316   islets, then reduced in the post-natal pig β-cell, a view supported by our quantification of

317   dynamic basal and glucose + IBMX regulation of insulin secretion at these stages (Fig. 6A).

318   Consistent with our observation that insulin secretion at basal glucose levels declined during

319   fetal to postnatal islet development, we observed that pathways involved in glucose processing

320   such as "glucose catabolic process", "ATP generation from ADP" and "calcium ion regulated

321   exocytosis" were down-regulated in β-cells (Fig. 6E). Compared to a relative peak in late fetal

322   development, transcripts of genes regulating glycolysis such as *ENO2, ALDOB, GPD1* and

323   *GCK* were down regulated by stage P22 (Fig. 6F). Thus, our data suggests that multiple inter-

324   related signaling pathways regulating insulin exocytosis continue to mature through weaning-

325   age (P22). In summary, our combined developmental, functional and molecular investigations

326   here revealed molecular and genetic factors governing maturation of neonatal β-cells and

327   unveiled conserved mechanisms underlying islet cell development and function in pigs and

328   humans.

329

330   **Discussion**

331   Based on the crucial role of pancreatic islets in human diseases and the expanding catalog of

332   differences between human and mouse islet developmental biology or regulation (Arda et al.,

333   2013; Arda et al., 2016; Brissova et al., 2005; Hart and Powers, 2019), there is intense interest in

334   developing complementary experimental systems for investigating islet development and

335   maturation. To address this need, we used an integrated approach to delineate pancreas

336   development in pigs. This multimodal assessment of genetic and developmental phenotypes

337   across a comprehensive range of fetal and post-natal stages of pig pancreas ontogeny and

338   maturation revealed multiple similarities in formation and regulation of pig and human islet β-, α-

339   and δ-cells, including features not observed in mice. Systematic phenotyping of pig pancreas

340   development - particularly gene expression and identification of developmental signaling

341   pathways - revealed unexpected dynamic gene regulation, and evidence of native intra-islet

342   GLP-1 signaling. Moreover, studies in pigs are cost-efficient (see Methods). Our experimental

11

343   approaches and findings provide a unique roadmap for diabetes and metabolic research,

344   including attempts to direct differentiation and maturation of replacement islet cell types from

345   renewable human cell sources.

346   Here, we established cell purification strategies based on flow cytometry to investigate

347   developmental genetics in fetal and neonatal pig β-, α- and δ-cells, an approach we and others

348   have successfully used in pancreas from mice and humans (Arda et al., 2016; Blodgett et al.,

349   2015; DiGruccio et al., 2016; Hrvatin et al., 2014a; Qiu et al., 2017). Like in prior studies (Arda

350   et al., 2016; Hrvatin et al., 2014a), we isolated primary β-, α- and δ-cells throughout fetal and

351   postnatal pancreas development using antibodies against hormones specific to these cell types,

352   an approach permitting comprehensive, high-quality stage-specific transcriptome analysis.

353   Similar approaches for primary ductal and acinar cells should provide opportunities in the future

354   to delineate the transcriptome of these important components of the exocrine pancreas.

355   Moreover, discovery of flow cytometry-based methods for purifying live primary endocrine or

356   exocrine cells, with antibodies that recognize cell-surface epitopes, should expand our capacity

357   to investigate other important aspects of pancreatic gene regulation and function, using

358   approaches like ATAC-Seq, promoter capture Hi-C, and Patch-Seq (Arda et al., 2018;

359   Camunas-Soler et al., 2019; Miguel-Escalada et al., 2019).

360   Transcriptome analysis described here provides evidence of genetic regulatory mechanisms

361   and cell development in pigs that are also conserved in other mammals, including (1) cell type-

362   specific expression of transcription factors (*PDX1, MAFA, ARX, IRX, HHEX*) and functional

363   regulators (*PCSK1, PCSK2, SLC2A2, SLC30A8, GLP1R, GCGR*), (2) transient β-, α- and δ-cell

364   proliferation, peaking in fetal/perinatal stages and regulated by conserved factors like *MKI67,*

365   *BUB1B* and *NUSAP1* (Georgia and Bhushan, 2004; Meier et al., 2008; Teta et al., 2007), (3)

366   dynamic expression of histone or chromatin regulators like *EZH2* and *DNMT1* (Chakravarthy et

367   al., 2017; Dai et al., 2017) and (4) reduction or elimination of transcripts encoding 'disallowed'

368   genes (Lemaire et al., 2017; Pullen et al., 2017; Pullen et al., 2010; Thorrez et al., 2011). These

369   findings from transcriptome analysis also correspond well with observations from our other

370   stage-specific tissue phenotyping (see below). Stage-specific gene expression patterns

371   revealed that pig and human β-cells and α-cells shared characteristic molecular and

372   developmental features not observed in mouse β-cells or α-cells. Like in human islets (Benner

373   et al., 2014), the transcription factor MAFB is expressed in both pig β- and α-cells (Figs. 2,3).

374   Similarly, we found that the transcription factor SIX3 is expressed in pig β-cells in an age-

375   dependent manner, like in human islets (Arda et al., 2016) (Fig. 3). Thus, studies of

376   mechanisms governing cell type- and age-dependent expression of genes like pig *MAFB* and

12

377 *SIX3* could reveal the basis of β-cell functional maturation. Likewise, we observed features of

378 pig fetal islets not yet noted in humans. *MAFA* expression in pig β-cells increased in fetal stages,

379 and continued through postnatal stages. In humans, β-cell *MAFA* expression begins in fetal

380 stages (Blodgett et al., 2015) and also increases after birth (Arda et al., 2016), but its fetal

381 regulation remains unreported. Our studies also provide a reference transcriptome analysis of

382 developing islet δ-cells, whose recognized role in health and diabetes is growing (Rorsman and

383 Huising, 2018). Together, the resources and methods described here provide evidence that

384 developmental genetic studies of pancreas in pigs could complement similar studies in humans

385 and mice.

386   In addition to the resemblance of pancreatic gene regulation in pigs and humans (Figs. 2,4),

387 we observed similarities of islet morphogenesis, cell specification, regulation and islet cell

388 allocation. Scattered islet β-, α- and δ-cells coalesced into small clusters at late fetal stages,

389 which contained proliferating cells (Figs. 2,3). At birth, the proportion of α- and δ-cells in pig

390 islets was ~50%, like that of neonatal human islets , and unlike in mice. In pig pancreas

391 development, a large portion of fetal hormone-expressing islet cells appeared to be contained

392 within small, dispersed clusters of varying cell composition. After birth, these clusters enlarged,

393 and the geometry of β-, α- and δ-cells in islets appeared intermingled, like in human islets

394 (Brissova et al., 2005) (Fig. 3). Studies of insulin secretion further demonstrated that β-cell

395 function matures from fetal to post-natal stages like in humans (Arda et al., 2016) and other

396 mammals. Thus, our study reveals multiple features in pig islet development that are closely

397 conserved in human pancreas, including a subset of phenotypes not observed in rodent islets,

398 suggesting that pigs could be a reliable surrogate animal model to study the islet function of

399 human gene orthologs. This includes studies of dominant forms of diabetes like MODY and

400 NDM, whose genetics have not been reconstituted in mice (Hattersley and Patel, 2017; Maestro

401 et al., 2007). By contrast, dominant monogenic diabetes resulting from mutations in *INS* or the

402 MODY3 gene *HNF1α* has been reconstituted in pigs (Renner et al., 2013; Umeyama et al.,

403 2009). Thus, studies of gene function and pathogenesis in diseases like MODY and NDM could

404 be advanced through investigations in pigs.

405   Here, we evaluated pancreas phenotypes through a full range of fetal and peri-natal stages.

406 In β-, α- and δ-cells, this 'granularity' of phenotyping revealed changes in >6000 genes during

407 development, and identified developmental dynamics not previously noted in studies of human

408 islet gene expression with comparatively limited sampling during developmental stages (Arda et

409 al., 2016; Blodgett et al., 2015; Bramswig et al., 2013), or in one study, a single stage (Ramond

13

410   et al., 2018). For example, in β-cells, genes involved in glucose processing, including *G6PC2*

411   and *PDK3*, are in the "Up_NC" cluster whereas genes regulating insulin secretion, such as

412   *SLC2A2*, are in the "NC_Up" cluster (Table S6), indicating that mechanisms governing glucose

413   sensing and metabolism, or insulin secretion, are established at different developmental stages

414   in pig β-cells. Moreover, we noted 366 β-cell or α-cell transcripts whose levels changed with a

415   'discontinuous' trajectory in development (Fig. 5 and Table S6). That is, we observed

416   heterogeneous patterns of expression, including early rise then fall (like *DPP4, FEV* in β-cells,

417   and *FOXO1* or *KIT* in α-cells), or initial decline followed by a later rise in transcript levels,

418   including those encoding a subset of disallowed gene products like PDK4 in β-cells (Fig. 5 and

419   Table S6). Thus, our ability to detect dynamic gene expression trajectories in β-cell or α-cells

420   was enhanced by the comprehensiveness of developmental phenotyping afforded in pigs.

421   Cell- and stage-specific phenotyping here also revealed links between our data to human

422   diabetes risk and islet replacement. Prior studies have noted a significant enrichment of

423   candidate diabetes risk genes among those with dynamic developmental expression (Arda et al.,

424   2016; Perez-Alcantara et al., 2018). Similarly, in our recent work, prioritization of candidate

425   diabetes risk genes with dynamic fetal or post-natal expression led to identification of SIX2,

426   SIX3 and BCL11A as unrecognized regulators of human β-cell development and function (Arda

427   et al., 2016; Peiris et al., 2018). Here, we found significant enrichment of β- and α-cell gene sets

428   involved in specific developmental signaling pathways (Fig. 5). Of these, only a subset, such as

429   mTOR, retinoic acid receptor and TGF-β signaling, have previously been linked to β- and α-cell

430   biology (Blandino-Rosano et al., 2017; Brun et al., 2015; Lin et al., 2009; Yokoi et al., 2016).

431   Thus, our datasets provide a foundation for systematic investigations of *cis-* and *trans-*

432   regulatory elements governing the dynamic expression of diabetes risk genes in the native,

433   physiological setting of pig islet development.

434   Identifying signals controlling islet development, including detection of signaling modulation,

435   should enhance efforts to control and direct differentiation of functional replacement islet cells

436   from stem cells and other renewable sources. Recent studies have explored use of neonatal pig

437   islet cultures for identifying signals that promote β-cell functional maturation (Hassouna et al.,

438   2018). In their work with stepwise directed differentiation of human stem cells into distinct

439   lineages, Loh and colleagues have demonstrated the value of inhibiting signaling pathways –

440   not merely through signal withdrawal, but by exposure of cells to potent signaling inhibitors – to

441   prevent development along undesired fates or lineages (Ang et al., 2018; Loh et al., 2014). The

442   identification of dynamically regulated genes and pathways, including those with discontinuous

14

443   trajectories (Up then Down, etc.), in β-cell and α-cell development provides a new roadmap for

444   modulating islet cell replacement efforts. Fetal and neonatal β-cells and α-cells develop in close

445   proximity, and our work likely identifies intercellular signaling pathways (like those regulated by

446   *PCSK1*, *GLP1R* and *DPP4*) that could regulate differentiation of these cells. PCSK1 expression

447   in mouse fetal α-cells was reported previously (Wilson et al., 2002) but active GLP-1 production

448   from fetal islets was not assessed; likewise, to our knowledge, human fetal islet GLP-1

449   production has not been reported. Recent studies have demonstrated that GLP1R can be

450   stimulated by glucagon, in addition to GLP-1 (Capozzi et al., 2019; Svendsen et al., 2018; Zhu

451   et al., 2019); however, it remains unknown if all signaling downstream of GLP1R is activated by

452   glucagon, or if islet cells are the sole target of GLP-1 signaling in the fetal pancreas. Further

453   studies of endogenous GLP-1 signaling in pig fetal islet development could also clarify the

454   emerging concept of intra-islet GLP-1 signaling in metabolically-stressed adult islets (Capozzi et

455   al., 2019; Drucker, 2013). Thus, our findings identify multiple pathways associated with fetal and

456   post-natal β-cell maturation or function (Table S9), including many not directly modulated in

457   prior studies (Nair et al., 2019; Pagliuca et al., 2014; Rezania et al., 2014; Russ et al., 2015). In

458   summary, data, conceptual advances and resources detailed here provide an unprecedented

459   molecular, cellular and developmental framework for investigating pancreas development that

460   could inform our understanding of diabetes and obesity risk, and advance efforts to produce

461   replacement human islets for diabetes.

462

Materials and methods

Animals and pancreas harvest

Pigs used in this study were outbred and used in accordance to protocols approved by the Institutional Animal Care and Use Committees at University of California Davis and Stanford University. For collection of fetal pig pancreata, pregnancies were confirmed via ultrasound 30 days after mating and pregnant gilts were humanely euthanized at 40, 70, or 90 days. The reproductive tracts were removed after mid-ventral laparotomy, cooled on ice, and fetuses were collected. Fetuses remained on ice until dissection. Pancreas was identified according to anatomical location and harvested under a stereoscopic microscope. Neonatal pancreata were harvested from neonatal piglets at 8 and 22 days of age, while adult pancreata were collected from pigs 6 months of age or older. Briefly, after euthanasia, a midline incision was performed to provide access to the peritoneum and thoracic cavity. The pancreas was rapidly chilled via either perfusion of sterile ice-cold saline solution into the descending aorta or by pouring the same solution directly into the peritoneal cavity and then surgically removed. Harvested pancreatic tissue was maintained at a temperature of 2-10°C in saline solution until further downstream processing.

Generation of pancreatic single cell suspensions

Morphological differences of the pancreas between developmental stages necessitated customized protocols to generate single cell suspensions suitable for downstream assays. Embryonic day 40 pancreata were diced finely with a razor blade and transferred into a 4°C solution of Collagenase D (Millipore-Sigma, Cat# C9263) at a concentration of 1 mg/ml in HBSS, and digested to single cells overnight at 4°C. Embryonic day 70 and 90 pancreata were finely diced with a razor blade and digested for 5-8 minutes at 37°C using the same Collagenase D solution above. The reaction was stopped with the addition of equal volume HBSS containing 10% porcine serum (Millipore-Sigma, Cat# P9783). If necessary, an additional digestion using TrypLE (Gibco, Cat#12605-010) for 3 minutes at 37°C was used to fully disperse any remaining cell clusters. Post-natal pancreata were digested following published methods (Lamb et al., 2014). (Logistical and technical challenges related to the mass of adult pigs precluded isolation of single cell islet suspensions of sufficient quality suitable for molecular analysis of adult pig islets.) Briefly, pancreata were trimmed to remove lymphatic, connective, and fat tissues, and chopped into 1-5 mm pieces. The tissue was digested using 2 mg/ml Collagenase D in HBSS at 37°C for 12-18 minutes. 1.5 volumes of HBSS with 10% porcine serum and 0.5% Antibiotic/Antimycotic solution was added to stop digestion. Neonatal Islet Cell clusters (NICCs)

16

497 of the desired size were obtained after straining digest through a 500 μm mesh (PluriSelect,

498 Cat# 43-50500-03) to remove large undigested tissue, washed, and allowed to gravity settle two

499 times. To generate single cell suspensions, some NICCs were further dispersed with TrypLE for

500 3 minutes at 37°C. Remaining NICCs were spun down and resuspended in RPMI 1640 (Gibco,

501 Cat# 11879-020) containing 5 mM glucose, 10% porcine serum, 10 mM HEPES (Caisson Labs,

502 HOL06-6X100ML) and 1% Pen/Strep (Life Technologies, Cat# 15140-122) and placed in a

503 humidified, 5% CO_2 tissue culture incubator.

504   The cost basis of pancreas procurement and islet isolation from pigs is currently lower than

505 for humans. In 2019, reimbursement for a single human cadaveric donor pancreas is between

506 $4,500 and $7,000 (US dollars). For human islets, investigators are charged $0.12 per islet

507 equivalent using the NIH-supported Integrated Islet Distribution Program (https://iidp.coh.org).

508 By contrast, the cost of a P22 pig pancreas is approximately $500, and after processing, a P22

509 pancreas yields approximately 90- to 100,000 NICCs. The total cost per pig NICC is <$0.008.

510

511 **Cell flow cytometry and purification**

512 Single cell suspensions were washed twice with cold PBS and filtered with a 70 μm filter (BD

513 Falcon, Cat# 352350). Prior to fixation, cells were stained with LIVE/DEAD fixable Aqua

514 (ThermoFisher, Cat# L34976) or LIVE/DEAD fixable Near-IR (ThermoFisher, Cat#L10119) dead

515 cell stains according to manufacturer's protocol. Cells were fixed with 4% PFA in PBS (Electron

516 Microscopy Sciences) for 10 minutes at room temperature. After fixation, cells were

517 permeabilized with Permeabilization Buffer: 1X PBS containing permeabilization solution

518 (BioLegend, Cat# 421002), 0.2% BSA (Sigma-Aldrich, Cat#A9576), mouse and rat IgG

519 (Jackson Labs, Cat# 015-000-003 and 012-000-003), and 1:40 Ribolock RNase Inhibitor (Fisher

520 Scientific, Cat# FEREO0384), for 30 minutes at 4°C. Cells were pelleted and resuspended with

521 Wash Buffer: 1X PBS containing permeabilization solution, 0.2% BSA, and 1:100 Ribolock.

522 Cells were pelleted again, supernatant removed, and stained with Alexa Fluor 488 labeled anti-

523 insulin (R&D Systems, IC1417G-100UG), Alexa Fluor 647 labeled anti-glucagon (Santa Cruz,

524 sc-57171 AF647) and PE labeled anti-somatostatin (Santa Cruz, sc-55565 PE) antibodies in

525 Staining Buffer: 1X PBS containing permeabilization solution, 1% BSA, and 1:40 Ribolock, for

526 30 minutes at 4°C. Cells were washed three times in Wash Buffer and resuspended in Sort

527 Buffer: 1X PBS containing 0.5% BSA, and 1:20 Ribolock. Labeled cells were sorted on a

528 special-order, 5-laser FACS Aria II using FACSDiva software (BD Biosciences). After excluding

529 doublets and dead cells, desired cell populations were identified using fluorescence minus one

530 (FMO) controls. Cells were sorted using the purity mask in chilled low retention tubes containing

17

531 50 µl of Sorting Buffer. We attempted to isolate cells producing more than one islet hormone

532 (insulin, glucagon or somatostatin) simultaneously, which have been reported in both human

533 and pig fetal pancreas (Lukinius et al., 1992; Riopel et al., 2014). In contrast to these studies,

534 however, the relative frequency of these cells after FACS was quite low (<0.001% of live cells)

535 and precluded downstream analysis. Similarly, the relative paucity of δ cells in the early fetal

536 porcine pancreas has proven a significant hurdle to collection of sufficient numbers for

537 downstream analysis. Post-hoc visualization of recorded data was performed using FlowJo vX

538 software (FlowJo, LLC).

539

540 **Total RNA extraction and quantitative Reverse Transcription PCR (qRT-PCR)**

541 Total RNA was extracted from the sorted cells as described (Hrvatin et al., 2014a) and

542 concentrated using the RNA Clean & Concentrator-5 kit (Zymo Research, Cat# R1013).

543 Complementary DNA (cDNA) was generated using the Maxima First Strand cDNA Synthesis kit

544 (Thermo Scientific, Cat# K1642) according to the manufacturer's instructions. Purity of sorted

545 populations was confirmed via Quantitative PCR using an Applied Biosystems 7500 Real-Time

546 PCR System.   The following TaqMan probes were used: INS (Ss03386682_u1), GCG

547 (Ss03384069_u1), SST (Ss03391856_m1), AMY2 (Ss03394345_m1), ACTB (Ss03376081_u1),

548 KRT19   (Forward: 5'-GAAGAGCTGGCCTACCTG-3',   Reverse: 5'-ATA

549 CTGGCTTCTCATGTCGC-3'), SIX2 (Forward: 5'-TCAAGGAAAAGAGTCGCAGC-3', Reverse:

550 5'-TGAACCAGTTGCTGACCTG-3') and SIX3 (Forward: 5'-AACAAGCACGAGTCGATCC-3',

551 Reverse: 5'-CCACAAGTTCACCAAGGAGT-3'). Relative mRNA abundance was calculated by

552 the Comparative Ct (ΔΔCt) relative quantitation method.

553

554 **RNA-Seq Library preparation**

555 Multiplexed libraries were prepared using the SMARTer Stranded Total RNA-Seq Kit v2 - Pico

556 Input Mammalian (TakaraBio, Cat# 634413) following manufacturer's instructions. Library

557 fragments of approximately 350 bp were obtained, and the quality was assessed using a 2100

558 Bioanalyzer (Agilent). Barcoded libraries were multiplexed and sequenced on an Illumina

559 NextSeq sequencer.

560

561 **Bioinformatic and statistical analysis of RNA-Seq datasets**

562 RNA-Seq libraries were sequenced as 75 bp pair-end reads to a depth of 30 to 60 million reads.

563 To estimate transcriptome abundance, Salmon algorithm (v0.11.3) was used (Patro et al.,

564 2017). An index was built on the Sus Scrofa reference transcriptome (Sscrofa 11.1, version 96)

565   (Zerbino et al., 2018) using Salmon with parameters "salmon index --keepDuplicates -t

566   transcripts -i transcripts_index --type quasi -k 31". The reads were aligned to the index and

567   quantified using Salmon with parameters "salmon quant -i $salmon_index -l A \-1 $Input1 \-2

568   $Input2 \ p 8 -o quants/${Input1}_quant \ --gcBias –seqBias". After getting the transcript counts,

569   differentially expressed gene analysis was performed using the DEseq2 analysis pipeline (Love

570   et al., 2014; Soneson et al., 2015). Differentially expressed genes (DEGs) were obtained by

571   comparisons of any two sequential stages (i.e. Early fetal versus Late fetal and Late fetal versus

572   Neonatal) in a cell type specific manner. Genes were considered differentially expressed if the

573   fold change between samples was greater than or equal to 1.5 with setting of Benjamini-

574   Hochberg (BH) false discovery rate (FDR) adjusted P value of <0.05 in the package.

575   Hierarchical clustering of samples were done with the cor() functions of R. Principal component

576   analysis (PCA) was performed with the function *plotPCA* that comes with DEseq2 package.

577   Visualization of RNA-seq data examined in this study were produced with pheatmap 1.0.12

578   (Kolde, 2012) and ggplot2 (Wickham, 2009). GO term analysis was carried out using the R

579   package clusterProfiler as described (Yu et al., 2012) with a Benjamini-Hochberg adjusted P

580   value of <0.1.

581

582   **Comparison to extant human and mouse β-cell transcriptomes**

583   Human (Arda et al., 2016; Blodgett et al., 2015) (GEO accession numbers GSE67543 and

584   GSE79469) and mouse (Qiu et al., 2017) (GEO accession number GSE87375) datasets were

585   obtained from the NCBI Gene Expression Omnibus (GEO). Indices for human and mouse

586   libraries were built from reference transcriptomes GRCh38 cDNA and GRCm38 cDNA,

587   respectively (Homo sapiens, version 96; Mus musculus, version 96; (Zerbino et al., 2018)). Pig

588   and mouse Ensembl IDs were converted to their corresponding human Ensembl ID using

589   predicted ortholog tables across these species obtained from Ensembl BioMart (Zerbino et al.,

590   2018). Sample-wise hierarchical clustering analysis (Fig. 4A) was performed using dist()

591   function of R.

592

593   **Identifying genes with dynamic expression**

594   To create lists of dynamically expressed genes, DEGs from comparisons between early fetal

595   and late fetal stages and between late fetal and neonatal stage were intersected, which created

596   lists of genes showing patterns of gene expression with up, down or no change directions as

597   development proceeds in islets development. Gene TPM values shifted by +1, log based 2

598 transformed were averaged across biological replicates and subsequently standardized to their
599 Z-scores.
600

Identification of developmentally regulated MODY and NDM genes

602   We queried 33 genes previously linked to MODY and/or NDM (Velayos et al., 2017; Yang
603 and Chan, 2016), and identified 19 dynamically expressed genes during the transition from fetal
604 to neonatal stages in pig β-, α- or δ-cells. Among these 19 candidates, we then used prior data
605 sets (Blodgett et al., 2015) to identify a subset that also have dynamic expression in human islet
606 β- or α-cells – a lack of available human δ-cell datasets precludes this comparison for δ-cells.
607

Immunohistochemistry

609 Biopsies of harvested pancreata were fixed in 4% paraformaldehyde (w/v) in PBS at 4°C
610 overnight, washed twice in PBS, and cryoprotected via sucrose saturation. The tissues were
611 imbedded in Tissue-Tek OCT compound (VWR, Cat# 25608-930) and stored at -80°C until
612 sectioning. 10μm thick sections were collected on ThermoFisher Superfrost Plus slides. For
613 staining, frozen slides were thawed at room temperature for 30 min and washed with PBS.
614 Antigen retrieval was performed by boiling slides immersed in Target Retrieval Solution (DAKO,
615 S169984-2) for 30 minutes, as needed. Subsequently, sections were incubated with
616 streptavidin/biotin blocking solution (Vector Labs, SP-2002) according to manufacturer's
617 instruction. Then, sections were incubated in permeabilization/blocking buffer (5% normal
618 donkey serum, 0.3% Triton X-100 in PBS) at room temperature for 1 hour followed by overnight
619 incubation at 4°C with primary antibodies diluted in Antibody dilution buffer (1% bovine serum
620 albumin, 0.3% Triton X-100 in PBS). Slides were washed and stained with appropriate
621 secondary antibodies for 1 hour at room temperature. Primary antibodies and dilutions used are
622 as follows: guinea pig anti-insulin (DAKO, A0564, 1:1000), mouse anti-glucagon (Sigma-Aldrich,
623 G2654, 1:1000), rabbit anti-SIX3 (LifeSpan Biosciences, LS-B9336, 1:100), goat anti-PDX1
624 (R&D systems, AF2419, 1:200), mouse anti-human NKX6.1 (R&D systems, AF5857, 1:200,)
625 rabbit anti-MAFB (Bethyl, IHC-00351, 1:200), rabbit anti-MAFA (AVIVA systems biology,
626 ARP47760_P050, 1:200), goat anti-somatostatin (Santa Cruz biotechnology, 1:500), rabbit anti-
627 Chromogranin A (Immunostar, 20085, 1:500), rat anti-E-cadherin (Life Technologies, 13-1900
628 1:500).   Secondary antibodies used are donkey anti-isotype conjugated with Alexa Fluor
629 488/555/647 (1:500; Molecular Probes). After a final wash with PBS, slides were preserved with
630 a mounting medium containing DAPI (Vector labs, H-1200) and coverslipped. Image acquisition
631 was performed on a Leica SP8 confocal microscope. Islet cells were quantified by counting

632   insulin positive β-cells, glucagon positive α-cells, and somatostatin positive δ-cells using

633   pancreas sections from different stages.

634

635   **Morphometric Analysis**

636   Tissue sections were prepared as above. Single-channel images were captured using a Zeiss

637   Axio Imager M2 microscope using a 20X objective with the AxioVision version 4.8 software.

638   Respective channel images were then imported into the Image-Pro Plus version 5 software

639   (Media Cybernetics, Inc.). Quantification of hormone^{+} cells was performed by using the count

640   function within the Measure menu. The number of individual hormone^{+} cells were then

641   summated for each developmental stage, and the fractional percentage comprising each of the

642   three cell types was calculated. To determine the percentage of β-, α-, and δ-cells which were

643   undergoing cell division at each developmental stage, slides were stained for a combination of

644   insulin, glucagon, and Ki67 or insulin, somatostatin, and Ki67. Single-channel images were

645   collected as above and then merged into a multi-channel image using the Image-Pro Plus

646   software. Cells which were Ki67^{+} and hormone[+], as well as the total number of hormone^{+} cells,

647   were then counted manually.

648

649   **In vitro insulin secretion assay**

650   Functional maturity of NICCs isolated from late fetal or 22-day old piglets was assessed by in

651   vitro glucose stimulated insulin secretion (GSIS) assay performed after 5 days of culture. In brief,

652   100 NICCs were washed and incubated at 2.8 mM glucose for 1 hour. After the initial

653   preincubation, clusters were serially incubated in media above containing 2.8 mM, 20 mM, and

654   20 mM plus IMBX glucose concentrations for 1 hour each. Finally, clusters were lysed in acid-

655   ethanol solution to extract the total insulin content. Insulin from supernatants and the NICC

656   lysates was quantified using the pig insulin ELISA kit (Mercodia, 10-12000-01). Secreted insulin

657   is presented as a percent of total insulin detected in lysate. All steps were performed in triplicate

658   at 37°C using RPMI 1640 supplemented with 2% porcine serum adjusted to the respective

659   glucose concentrations.

660

661   **In vitro active GLP-1 assay**

662   Islet cell clusters were handpicked immediately after isolation, washed twice in ice cold PBS,

663   then resuspended in 4°C lysis buffer containing DPP4 inhibitor (EMD Millipore, DPP4). Clusters

664   were sonicated at 4°C and immediately stored at -80°C. Active GLP-1 (7-36) was measured

665   using the Mouse / Rat GLP-1 Active (7-36) ELISA Kit (Eagle Biosciences, GP121-K01).

666

Statistical analysis

667

668 For qRT-PCR, GSIS and quantification of immunohistology experiments, the number of

669 biological or technical replicates (n), measure of central tendency (e.g. average), standard

670 deviation (SD), and statistical analysis is detailed in the Figure legend. Graphs and statistical

671 analysis were produced and performed by using GraphPad Prism (version 8) software.

672

673 **Acknowledgements**

674 We thank past and current members of the Kim group for advice and encouragement, Dr. Sam

675 Baker (Stanford, Dept. of Comparative Medicine, Veterinary Service Center), Dr. Jing Wang

676 (Stanford Diabetes Research Center and Stanford Islet Research Core) and Michael Alexander

677 (U.C. Irvine) for assistance with pig pancreas work, Serena Whitener for help developing the pig

678 pancreas gene expression browser, Dr. Kyle Loh for stimulating discussions, and Drs. Dan Lu

679 and Ramesh Nair for help on bioinformatics.

680

681 **Competing interests:** Nothing to declare

682

683 **Funding**

684 This work was supported by a Deans Innovation Fund from the Dept. of Developmental Biology

685 (Stanford), and by fellowship awards from the L.L. Hillblom Foundation (2017-D-008-FEL) to

686 S.K., from the Division of Endocrinology T32 training grant (DK007217-41, A. Hoffman and F.

687 Kraemer) to R.L.W., and from the Stanford Child Health Research Institute (UL1 TR001085)

688 and the American Diabetes Association (1-16-PDF-086) to H.P. Work in the Kim lab was also

689 supported by grants from the U.S. National Institutes of Health P30 DK116074, and by the

690 Stanford Islet Research Core and Diabetes Genomics and Analysis Core of Stanford Diabetes

691 Research Center.

692

693 **Data Availability**

694 The data discussed in this publication have been deposited in NCBI's Gene Expression

695 Omnibus (Edgar et al., 2002) and are accessible through GEO Series accession number

696 GSE143889 (https://www.ncbi.nlm.nih.gov/geo/query/acc.cgi?acc= GSE143889).

697

698 **Requests for materials & correspondence** should be addressed to Seung K. Kim.

699

22

700 **Author contributions**

701 S.K., R.L.W. and S.K.K. designed the study; S.K, R.L.W, X.G., C.A.C., J.Y.L., I.P., R.J.B., and

702 K.T. performed the experiments; J.C., S.R.Q., J.R.T.L., R.B., and P.J.R. shared materials; S.K.,

703 R.L.W., H.P., and S.K.K analyzed the data and wrote the manuscript.

References

Aguayo-Mazzucato, C., Koh, A., El Khattabi, I., Li, W. C., Toschi, E., Jermendy, A., Juhl, K., Mao, K., Weir, G. C., Sharma, A., et al. (2011). Mafa expression enhances glucose-responsive insulin secretion in neonatal rat beta cells. *Diabetologia* **54**, 583-593.

Ang, L. T., Tan, A. K. Y., Autio, M. I., Goh, S. H., Choo, S. H., Lee, K. L., Tan, J., Pan, B., Lee, J. J. H., Lum, J. J., et al. (2018). A Roadmap for Human Liver Differentiation from Pluripotent Stem Cells. *Cell Rep* **22**, 2190-2205.

Arda, H. E., Benitez, C. M. and Kim, S. K. (2013). Gene regulatory networks governing pancreas development. *Dev Cell* **25**, 5-13.

Arda, H. E., Li, L., Tsai, J., Torre, E. A., Rosli, Y., Peiris, H., Spitale, R. C., Dai, C., Gu, X., Qu, K., et al. (2016). Age-Dependent Pancreatic Gene Regulation Reveals Mechanisms Governing Human beta Cell Function. *Cell metabolism* **23**, 909-920.

Arda, H. E., Tsai, J., Rosli, Y. R., Giresi, P., Bottino, R., Greenleaf, W. J., Chang, H. Y. and Kim, S. K. (2018). A Chromatin Basis for Cell Lineage and Disease Risk in the Human Pancreas. *Cell Syst* **7**, 310-322 e314.

Artner, I., Blanchi, B., Raum, J. C., Guo, M., Kaneko, T., Cordes, S., Sieweke, M. and Stein, R. (2007). MafB is required for islet beta cell maturation. *Proc Natl Acad Sci U S A* **104**, 3853-3858.

Artner, I., Hang, Y., Mazur, M., Yamamoto, T., Guo, M., Lindner, J., Magnuson, M. A. and Stein, R. (2010). MafA and MafB regulate genes critical to beta-cells in a unique temporal manner. *Diabetes* **59**, 2530-2539.

Avrahami, D., Li, C., Zhang, J., Schug, J., Avrahami, R., Rao, S., Stadler, M. B., Burger, L., Schubeler, D., Glaser, B., et al. (2015). Aging-Dependent Demethylation of Regulatory Elements Correlates with Chromatin State and Improved beta Cell Function. *Cell metabolism* **22**, 619-632.

Benner, C., van der Meulen, T., Caceres, E., Tigyi, K., Donaldson, C. J. and Huising, M. O. (2014). The transcriptional landscape of mouse beta cells compared to human beta cells reveals notable species differences in long non-coding RNA and protein-coding gene expression. *BMC Genomics* **15**, 620.

Blandino-Rosano, M., Barbaresso, R., Jimenez-Palomares, M., Bozadjieva, N., Werneck-de-Castro, J. P., Hatanaka, M., Mirmira, R. G., Sonenberg, N., Liu, M., Ruegg, M. A., et al. (2017). Loss of mTORC1 signalling impairs beta-cell homeostasis and insulin processing. *Nat Commun* **8**, 16014.

Blodgett, D. M., Nowosielska, A., Afik, S., Pechhold, S., Cura, A. J., Kennedy, N. J., Kim, S., Kucukural, A., Davis, R. J., Kent, S. C., et al. (2015). Novel Observations From Next-Generation RNA Sequencing of Highly Purified Human Adult and Fetal Islet Cell Subsets. *Diabetes* **64**, 3172-3181.

Blum, B., Hrvatin, S., Schuetz, C., Bonal, C., Rezania, A. and Melton, D. A. (2012). Functional beta-cell maturation is marked by an increased glucose threshold and by expression of urocortin 3. *Nat Biotechnol* **30**, 261-264.

Bramswig, N. C., Everett, L. J., Schug, J., Dorrell, C., Liu, C., Luo, Y., Streeter, P. R., Naji, A., Grompe, M. and Kaestner, K. H. (2013). Epigenomic plasticity enables human pancreatic alpha to beta cell reprogramming. *J Clin Invest* **123**, 1275-1284.

Brissova, M., Fowler, M. J., Nicholson, W. E., Chu, A., Hirshberg, B., Harlan, D. M. and Powers, A. C. (2005). Assessment of human pancreatic islet architecture and composition by laser scanning confocal microscopy. *J Histochem Cytochem* **53**, 1087-1097.

Brun, P. J., Grijalva, A., Rausch, R., Watson, E., Yuen, J. J., Das, B. C., Shudo, K., Kagechika, H., Leibel, R. L. and Blaner, W. S. (2015). Retinoic acid receptor signaling is required to maintain glucose-stimulated insulin secretion and beta-cell mass. *FASEB J* **29**, 671-683.

755 **Camunas-Soler, J., Dai, X., Hang, Y., Bautista, A., Lyon, J., Suzuki, K., Kim, S. K., Quake,**
756 **S. R. and MacDonald, P. E.** (2019). Pancreas patch-seq links physiologic dysfunction in
757 diabetes to single-cell transcriptomic phenotypes. *bioRxiv*, 555110.
758 **Capozzi, M. E., Svendsen, B., Encisco, S. E., Lewandowski, S. L., Martin, M. D., Lin, H.,**
759 **Jaffe, J. L., Coch, R. W., Haldeman, J. M., MacDonald, P. E., et al.** (2019). beta Cell tone
760 is defined by proglucagon peptides through cAMP signaling. *JCI Insight* **4**.
761 **Carlsson, G. L., Heller, R. S., Serup, P. and Hyttel, P.** (2010). Immunohistochemistry of
762 pancreatic development in cattle and pig. *Anat Histol Embryol* **39**, 107-119.
763 **Cerolsaletti, K., Hao, W. and Greenbaum, C. J.** (2019). Genetics Coming of Age in Type 1
764 Diabetes. *Diabetes Care* **42**, 189-191.
765 **Chakravarthy, H., Gu, X., Enge, M., Dai, X., Wang, Y., Damond, N., Downie, C., Liu, K.,**
766 **Wang, J., Xing, Y., et al.** (2017). Converting Adult Pancreatic Islet alpha Cells into beta
767 Cells by Targeting Both Dnmt1 and Arx. *Cell metabolism* **25**, 622-634.
768 **Collombat, P., Mansouri, A., Hecksher-Sorensen, J., Serup, P., Krull, J., Gradwohl, G. and**
769 **Gruss, P.** (2003). Opposing actions of Arx and Pax4 in endocrine pancreas development.
770 *Genes Dev* **17**, 2591-2603.
771 **Dai, C., Hang, Y., Shostak, A., Poffenberger, G., Hart, N., Prasad, N., Phillips, N., Levy, S.**
772 **E., Greiner, D. L., Shultz, L. D., et al.** (2017). Age-dependent human beta cell proliferation
773 induced by glucagon-like peptide 1 and calcineurin signaling. *J Clin Invest* **127**, 3835-3844.
774 **DiGruccio, M. R., Mawla, A. M., Donaldson, C. J., Noguchi, G. M., Vaughan, J., Cowing-**
775 **Zitron, C., van der Meulen, T. and Huising, M. O.** (2016). Comprehensive alpha, beta and
776 delta cell transcriptomes reveal that ghrelin selectively activates delta cells and promotes
777 somatostatin release from pancreatic islets. *Mol Metab* **5**, 449-458.
778 **Drucker, D. J.** (2013). Incretin action in the pancreas: potential promise, possible perils, and
779 pathological pitfalls. *Diabetes* **62**, 3316-3323.
780 **Dyson, M. C., Alloosh, M., Vuchetich, J. P., Mokelke, E. A. and Sturek, M.** (2006).
781 Components of metabolic syndrome and coronary artery disease in female Ossabaw swine
782 fed excess atherogenic diet. *Comp Med* **56**, 35-45.
783 **Edgar, R., Domrachev, M. and Lash, A. E.** (2002). Gene Expression Omnibus: NCBI gene
784 expression and hybridization array data repository. *Nucleic Acids Res* **30**, 207-210.
785 **Ferrer, J., Scott, W. E., 3rd, Weegman, B. P., Suszynski, T. M., Sutherland, D. E., Hering,**
786 **B. J. and Papas, K. K.** (2008). Pig pancreas anatomy: implications for pancreas
787 procurement, preservation, and islet isolation. *Transplantation* **86**, 1503-1510.
788 **Fisher, J. E., Lillegard, J. B., McKenzie, T. J., Rodysill, B. R., Wettstein, P. J. and Nyberg,**
789 **S. L.** (2013). In utero transplanted human hepatocytes allow postnatal engraftment of
790 human hepatocytes in pigs. *Liver transplantation : official publication of the American*
791 *Association for the Study of Liver Diseases and the International Liver Transplantation*
792 *Society* **19**, 328-335.
793 **Georgia, S. and Bhushan, A.** (2004). Beta cell replication is the primary mechanism for
794 maintaining postnatal beta cell mass. *J Clin Invest* **114**, 963-968.
795 **Hart, N. J. and Powers, A. C.** (2019). Use of human islets to understand islet biology and
796 diabetes: progress, challenges and suggestions. *Diabetologia* **62**, 212-222.
797 **Hassouna, T., Seeberger, K. L., Salama, B. and Korbutt, G. S.** (2018). Functional Maturation
798 and In Vitro Differentiation of Neonatal Porcine Islet Grafts. *Transplantation* **102**, e413-
799 e423.
800 **Hattersley, A. T. and Patel, K. A.** (2017). Precision diabetes: learning from monogenic
801 diabetes. *Diabetologia* **60**, 769-777.
802 **Holst, J. J., Holland, W., Gromada, J., Lee, Y., Unger, R. H., Yan, H., Sloop, K. W., Kieffer,**
803 **T. J., Damond, N. and Herrera, P. L.** (2017). Insulin and Glucagon: Partners for Life.
804 *Endocrinology* **158**, 696-701.

805 **Hrvatin, S., Deng, F., O'Donnell, C. W., Gifford, D. K. and Melton, D. A.** (2014a). MARIS:
806   method for analyzing RNA following intracellular sorting. *PLoS One* **9**, e89459.
807 **Hrvatin, S., O'Donnell, C. W., Deng, F., Millman, J. R., Pagliuca, F. W., Dilorio, P., Rezania,**
808   **A., Gifford, D. K. and Melton, D. A.** (2014b). Differentiated human stem cells resemble
809   fetal, not adult, β cells. *Proceedings of the National Academy of Sciences* **111**, 3038.
810 **Jeon, J., Correa-Medina, M., Ricordi, C., Edlund, H. and Diez, J. A.** (2009). Endocrine cell
811   clustering during human pancreas development. *J Histochem Cytochem* **57**, 811-824.
812 **Jorgensen, M. C., Ahnfelt-Ronne, J., Hald, J., Madsen, O. D., Serup, P. and Hecksher-**
813   **Sorensen, J.** (2007). An illustrated review of early pancreas development in the mouse.
814   *Endocr Rev* **28**, 685-705.
815 **Kemter, E., Cohrs, C. M., Schafer, M., Schuster, M., Steinmeyer, K., Wolf-van Buerck, L.,**
816   **Wolf, A., Wuensch, A., Kurome, M., Kessler, B., et al.** (2017). INS-eGFP transgenic pigs:
817   a novel reporter system for studying maturation, growth and vascularisation of neonatal
818   islet-like cell clusters. *Diabetologia* **60**, 1152-1156.
819 **Kolde, R.** (2012). Pheatmap: pretty heatmaps. *R package version* **61**, 617.
820 **Lamb, M., Laugenour, K., Liang, O., Alexander, M., Foster, C. E. and Lakey, J. R.** (2014). In
821   vitro maturation of viable islets from partially digested young pig pancreas. *Cell Transplant*
822   **23**, 263-272.
823 **Lee, Y. H., Wang, M. Y., Yu, X. X. and Unger, R. H.** (2016). Glucagon is the key factor in the
824   development of diabetes. *Diabetologia* **59**, 1372-1375.
825 **Lemaire, K., Granvik, M., Schraenen, A., Goyvaerts, L., Van Lommel, L., Gomez-Ruiz, A.,**
826   **In 't Veld, P., Gilon, P. and Schuit, F.** (2017). How stable is repression of disallowed
827   genes in pancreatic islets in response to metabolic stress? *PLoS One* **12**, e0181651.
828 **Lemaire, K., Thorrez, L. and Schuit, F.** (2016). Disallowed and Allowed Gene Expression:
829   Two Faces of Mature Islet Beta Cells. *Annu Rev Nutr* **36**, 45-71.
830 **Lim, H., Lim, Y. M., Kim, K. H., Jeon, Y. E., Park, K., Kim, J., Hwang, H. Y., Lee, D. J.,**
831   **Pagire, H., Kwon, H. J., et al.** (2018). A novel autophagy enhancer as a therapeutic agent
832   against metabolic syndrome and diabetes. *Nat Commun* **9**, 1438.
833 **Lin, H. M., Lee, J. H., Yadav, H., Kamaraju, A. K., Liu, E., Zhigang, D., Vieira, A., Kim, S. J.,**
834   **Collins, H., Matschinsky, F., et al.** (2009). Transforming growth factor-beta/Smad3
835   signaling regulates insulin gene transcription and pancreatic islet beta-cell function. *J Biol*
836   *Chem* **284**, 12246-12257.
837 **Loh, K. M., Ang, L. T., Zhang, J., Kumar, V., Ang, J., Auyeong, J. Q., Lee, K. L., Choo, S.**
838   **H., Lim, C. Y., Nichane, M., et al.** (2014). Efficient endoderm induction from human
839   pluripotent stem cells by logically directing signals controlling lineage bifurcations. *Cell Stem*
840   *Cell* **14**, 237-252.
841 **Love, M. I., Huber, W. and Anders, S.** (2014). Moderated estimation of fold change and
842   dispersion for RNA-seq data with DESeq2. *Genome Biol* **15**, 550.
843 **Lukinius, A., Ericsson, J. L., Grimelius, L. and Korsgren, O.** (1992). Ultrastructural studies of
844   the ontogeny of fetal human and porcine endocrine pancreas, with special reference to
845   colocalization of the four major islet hormones. *Dev Biol* **153**, 376-385.
846 **Maestro, M. A., Cardalda, C., Boj, S. F., Luco, R. F., Servitja, J. M. and Ferrer, J.** (2007).
847   Distinct roles of HNF1beta, HNF1alpha, and HNF4alpha in regulating pancreas
848   development, beta-cell function and growth. *Endocr Dev* **12**, 33-45.
849 **Matsunari, H., Nagashima, H., Watanabe, M., Umeyama, K., Nakano, K., Nagaya, M.,**
850   **Kobayashi, T., Yamaguchi, T., Sumazaki, R., Herzenberg, L. A., et al.** (2013). Blastocyst
851   complementation generates exogenic pancreas in vivo in apancreatic cloned pigs. *Proc Natl*
852   *Acad Sci U S A* **110**, 4557-4562.
853 **McKnight, K. D., Wang, P. and Kim, S. K.** (2010). Deconstructing pancreas development to
854   reconstruct human islets from pluripotent stem cells. *Cell Stem Cell* **6**, 300-308.

26

855 **Meier, J. J., Butler, A. E., Saisho, Y., Monchamp, T., Galasso, R., Bhushan, A., Rizza, R. A.**
856 **and Butler, P. C.** (2008). Beta-cell replication is the primary mechanism subserving the
857 postnatal expansion of beta-cell mass in humans. *Diabetes* **57**, 1584-1594.
858 **Miguel-Escalada, I., Bonas-Guarch, S., Cebola, I., Ponsa-Cobas, J., Mendieta-Esteban, J.,**
859 **Atla, G., Javierre, B. M., Rolando, D. M. Y., Farabella, I., Morgan, C. C., et al.** (2019).
860 Human pancreatic islet three-dimensional chromatin architecture provides insights into the
861 genetics of type 2 diabetes. *Nat Genet* **51**, 1137-1148.
862 **Mueller, K. R., Balamurugan, A. N., Cline, G. W., Pongratz, R. L., Hooper, R. L., Weegman,**
863 **B. P., Kitzmann, J. P., Taylor, M. J., Graham, M. L., Schuurman, H. J., et al.** (2013).
864 Differences in glucose-stimulated insulin secretion in vitro of islets from human, nonhuman
865 primate, and porcine origin. *Xenotransplantation* **20**, 75-81.
866 **Muraro, M. J., Dharmadhikari, G., Grun, D., Groen, N., Dielen, T., Jansen, E., van Gurp, L.,**
867 **Engelse, M. A., Carlotti, F., de Koning, E. J., et al.** (2016). A Single-Cell Transcriptome
868 Atlas of the Human Pancreas. *Cell Syst* **3**, 385-394 e383.
869 **Nagaya, M., Hayashi, A., Nakano, K., Honda, M., Hasegawa, K., Okamoto, K., Itazaki, S.,**
870 **Matsunari, H., Watanabe, M., Umeyama, K., et al.** (2019). Distributions of endocrine cell
871 clusters during porcine pancreatic development. *PLoS One* **14**, e0216254.
872 **Nair, G. G., Liu, J. S., Russ, H. A., Tran, S., Saxton, M. S., Chen, R., Juang, C., Li, M. L.,**
873 **Nguyen, V. Q., Giacometti, S., et al.** (2019). Recapitulating endocrine cell clustering in
874 culture promotes maturation of human stem-cell-derived beta cells. *Nat Cell Biol* **21**, 263-
875 274.
876 **Pagliuca, F. W., Millman, J. R., Gurtler, M., Segel, M., Van Dervort, A., Ryu, J. H., Peterson,**
877 **Q. P., Greiner, D. and Melton, D. A.** (2014). Generation of functional human pancreatic
878 beta cells in vitro. *Cell* **159**, 428-439.
879 **Pan, F. C. and Brissova, M.** (2014). Pancreas development in humans. *Current opinion in*
880 *endocrinology, diabetes, and obesity* **21**, 77-82.
881 **Patro, R., Duggal, G., Love, M. I., Irizarry, R. A. and Kingsford, C.** (2017). Salmon provides
882 fast and bias-aware quantification of transcript expression. *Nat Methods* **14**, 417-419.
883 **Pearson, E. R.** (2019). Type 2 diabetes: a multifaceted disease. *Diabetologia* **62**, 1107-1112.
884 **Peiris, H., Park, S., Louis, S., Gu, X., Lam, J. Y., Asplund, O., Ippolito, G. C., Bottino, R.,**
885 **Groop, L., Tucker, H., et al.** (2018). Discovering human diabetes-risk gene function with
886 genetics and physiological assays. *Nat Commun* **9**, 3855.
887 **Perez-Alcantara, M., Honore, C., Wesolowska-Andersen, A., Gloyn, A. L., McCarthy, M. I.,**
888 **Hansson, M., Beer, N. L. and van de Bunt, M.** (2018). Patterns of differential gene
889 expression in a cellular model of human islet development, and relationship to type 2
890 diabetes predisposition. *Diabetologia* **61**, 1614-1622.
891 **Pullen, T. J., Huising, M. O. and Rutter, G. A.** (2017). Analysis of Purified Pancreatic Islet
892 Beta and Alpha Cell Transcriptomes Reveals 11beta-Hydroxysteroid Dehydrogenase
893 (Hsd11b1) as a Novel Disallowed Gene. *Front Genet* **8**, 41.
894 **Pullen, T. J., Khan, A. M., Barton, G., Butcher, S. A., Sun, G. and Rutter, G. A.** (2010).
895 Identification of genes selectively disallowed in the pancreatic islet. *Islets* **2**, 89-95.
896 **Qiu, W.-L., Zhang, Y.-W., Feng, Y., Li, L.-C., Yang, L. and Xu, C.-R.** (2017). Deciphering
897 Pancreatic Islet β Cell and α Cell Maturation Pathways and Characteristic Features at the
898 Single-Cell Level. *Cell metabolism* **25**, 1194-1205.e1194.
899 **Ramond, C., Beydag-Tasoz, B. S., Azad, A., van de Bunt, M., Petersen, M. B. K., Beer, N.**
900 **L., Glaser, N., Berthault, C., Gloyn, A. L., Hansson, M., et al.** (2018). Understanding
901 human fetal pancreas development using subpopulation sorting, RNA sequencing and
902 single-cell profiling. *Development* **145**.
903 **Renner, S., Braun-Reichhart, C., Blutke, A., Herbach, N., Emrich, D., Streckel, E., Wunsch,**
904 **A., Kessler, B., Kurome, M., Bahr, A., et al.** (2013). Permanent neonatal diabetes in
905 INS(C94Y) transgenic pigs. *Diabetes* **62**, 1505-1511.

906 **Rezania, A., Bruin, J. E., Arora, P., Rubin, A., Batushansky, I., Asadi, A., O'Dwyer, S.,**
907   **Quiskamp, N., Mojibian, M., Albrecht, T., et al.** (2014). Reversal of diabetes with insulin-
908   producing cells derived in vitro from human pluripotent stem cells. *Nat Biotechnol* **32**, 1121-
909   1133.
910 **Riopel, M., Li, J., Fellows, G. F., Goodyer, C. G. and Wang, R.** (2014). Ultrastructural and
911   immunohistochemical analysis of the 8-20 week human fetal pancreas. *Islets* **6**, e982949.
912 **Rorsman, P., Berggren, P. O., Bokvist, K., Ericson, H., Mohler, H., Ostenson, C. G. and**
913   **Smith, P. A.** (1989). Glucose-inhibition of glucagon secretion involves activation of GABAA-
914   receptor chloride channels. *Nature* **341**, 233-236.
915 **Rorsman, P. and Huising, M. O.** (2018). The somatostatin-secreting pancreatic delta-cell in
916   health and disease. *Nat Rev Endocrinol* **14**, 404-414.
917 **Rouille, Y., Martin, S. and Steiner, D. F.** (1995). Differential processing of proglucagon by the
918   subtilisin-like prohormone convertases PC2 and PC3 to generate either glucagon or
919   glucagon-like peptide. *J Biol Chem* **270**, 26488-26496.
920 **Russ, H. A., Parent, A. V., Ringler, J. J., Hennings, T. G., Nair, G. G., Shveygert, M., Guo,**
921   **T., Puri, S., Haataja, L., Cirulli, V., et al.** (2015). Controlled induction of human pancreatic
922   progenitors produces functional beta-like cells in vitro. *The EMBO journal* **34**, 1759-1772.
923 **Sanyoura, M., Philipson, L. H. and Naylor, R.** (2018). Monogenic Diabetes in Children and
924   Adolescents: Recognition and Treatment Options. *Curr Diab Rep* **18**, 58.
925 **Schaffer, A. E., Taylor, B. L., Benthuysen, J. R., Liu, J., Thorel, F., Yuan, W., Jiao, Y.,**
926   **Kaestner, K. H., Herrera, P. L., Magnuson, M. A., et al.** (2013). Nkx6.1 controls a gene
927   regulatory network required for establishing and maintaining pancreatic Beta cell identity.
928   *PLoS Genet* **9**, e1003274.
929 **Sekine, N., Cirulli, V., Regazzi, R., Brown, L. J., Gine, E., Tamarit-Rodriguez, J., Girotti, M.,**
930   **Marie, S., MacDonald, M. J., Wollheim, C. B., et al.** (1994). Low lactate dehydrogenase
931   and high mitochondrial glycerol phosphate dehydrogenase in pancreatic beta-cells.
932   Potential role in nutrient sensing. *J Biol Chem* **269**, 4895-4902.
933 **Sheets, T. P., Park, K. E., Park, C. H., Swift, S. M., Powell, A., Donovan, D. M. and Telugu,**
934   **B. P.** (2018). Targeted Mutation of NGN3 Gene Disrupts Pancreatic Endocrine Cell
935   Development in Pigs. *Sci Rep* **8**, 3582.
936 **Sneddon, J. B., Tang, Q., Stock, P., Bluestone, J. A., Roy, S., Desai, T. and Hebrok, M.**
937   (2018). Stem Cell Therapies for Treating Diabetes: Progress and Remaining Challenges.
938   *Cell Stem Cell* **22**, 810-823.
939 **Sodoyez-Goffaux, F., Sodoyez, J. C., De Vos, C. J. and Foa, P. P.** (1979). Insulin and
940   glucagon secretion by islets isolated from fetal and neonatal rats. *Diabetologia* **16**, 121-123.
941 **Soneson, C., Love, M. I. and Robinson, M. D.** (2015). Differential analyses for RNA-seq:
942   transcript-level estimates improve gene-level inferences. *F1000Res* **4**, 1521.
943 **Steiner, D. F.** (1998). The proprotein convertases. *Curr Opin Chem Biol* **2**, 31-39.
944 **Sugiyama, T., Benitez, C. M., Ghodasara, A., Liu, L., McLean, G. W., Lee, J., Blauwkamp,**
945   **T. A., Nusse, R., Wright, C. V., Gu, G., et al.** (2013). Reconstituting pancreas development
946   from purified progenitor cells reveals genes essential for islet differentiation. *Proc Natl Acad*
947   *Sci U S A* **110**, 12691-12696.
948 **Svendsen, B., Larsen, O., Gabe, M. B. N., Christiansen, C. B., Rosenkilde, M. M., Drucker,**
949   **D. J. and Holst, J. J.** (2018). Insulin Secretion Depends on Intra-islet Glucagon Signaling.
950   *Cell Rep* **25**, 1127-1134 e1122.
951 **Tengholm, A. and Gylfe, E.** (2017). cAMP signalling in insulin and glucagon secretion.
952   *Diabetes Obes Metab* **19 Suppl 1**, 42-53.
953 **Teta, M., Rankin, M. M., Long, S. Y., Stein, G. M. and Kushner, J. A.** (2007). Growth and
954   regeneration of adult beta cells does not involve specialized progenitors. *Dev Cell* **12**, 817-
955   826.

956   **Thorrez, L., Laudadio, I., Van Deun, K., Quintens, R., Hendrickx, N., Granvik, M., Lemaire,**
957   **K., Schraenen, A., Van Lommel, L., Lehnert, S., et al.** (2011). Tissue-specific
958   disallowance of housekeeping genes: the other face of cell differentiation. *Genome Res* **21**,
959   95-105.
960   **Umeyama, K., Watanabe, M., Saito, H., Kurome, M., Tohi, S., Matsunari, H., Miki, K. and**
961   **Nagashima, H.** (2009). Dominant-negative mutant hepatocyte nuclear factor 1alpha
962   induces diabetes in transgenic-cloned pigs. *Transgenic Res* **18**, 697-706.
963   **van der Meulen, T., Donaldson, C. J., Caceres, E., Hunter, A. E., Cowing-Zitron, C., Pound,**
964   **L. D., Adams, M. W., Zembrzycki, A., Grove, K. L. and Huising, M. O.** (2015). Urocortin3
965   mediates somatostatin-dependent negative feedback control of insulin secretion. *Nat Med*
966   **21**, 769-776.
967   **Velayos, T., Martinez, R., Alonso, M., Garcia-Etxebarria, K., Aguayo, A., Camarero, C.,**
968   **Urrutia, I., Martinez de LaPiscina, I., Barrio, R., Santin, I., et al.** (2017). An Activating
969   Mutation in STAT3 Results in Neonatal Diabetes Through Reduced Insulin Synthesis.
970   *Diabetes* **66**, 1022-1029.
971   **Wende, A. R., Huss, J. M., Schaeffer, P. J., Giguere, V. and Kelly, D. P.** (2005). PGC-1alpha
972   coactivates PDK4 gene expression via the orphan nuclear receptor ERRalpha: a
973   mechanism for transcriptional control of muscle glucose metabolism. *Mol Cell Biol* **25**,
974   10684-10694.
975   **Wickham, H.** (2009). ggplot2: Elegant Graphics for Data Analysis. *Use R*, 1-212.
976   **Wilson, M. E., Kalamaras, J. A. and German, M. S.** (2002). Expression pattern of IAPP and
977   prohormone convertase 1/3 reveals a distinctive set of endocrine cells in the embryonic
978   pancreas. *Mech Dev* **115**, 171-176.
979   **Wu, J., Platero-Luengo, A., Sakurai, M., Sugawara, A., Gil, M. A., Yamauchi, T., Suzuki, K.,**
980   **Bogliotti, Y. S., Cuello, C., Morales Valencia, M., et al.** (2017). Interspecies Chimerism
981   with Mammalian Pluripotent Stem Cells. *Cell* **168**, 473-486 e415.
982   **Yang, Y. and Chan, L.** (2016). Monogenic Diabetes: What It Teaches Us on the Common
983   Forms of Type 1 and Type 2 Diabetes. *Endocr Rev* **37**, 190-222.
984   **Yokoi, N., Gheni, G., Takahashi, H. and Seino, S.** (2016). beta-Cell glutamate signaling: Its
985   role in incretin-induced insulin secretion. *J Diabetes Investig* **7 Suppl 1**, 38-43.
986   **Yu, G., Wang, L. G., Han, Y. and He, Q. Y.** (2012). clusterProfiler: an R package for comparing
987   biological themes among gene clusters. *OMICS* **16**, 284-287.
988   **Zerbino, D. R., Achuthan, P., Akanni, W., Amode, M. R., Barrell, D., Bhai, J., Billis, K.,**
989   **Cummins, C., Gall, A., Giron, C. G., et al.** (2018). Ensembl 2018. *Nucleic Acids Res* **46**,
990   D754-D761.
991   **Zhu, L., Dattaroy, D., Pham, J., Wang, L., Barella, L. F., Cui, Y., Wilkins, K. J., Roth, B. L.,**
992   **Hochgeschwender, U., Matschinsky, F. M., et al.** (2019). Intra-islet glucagon signaling is
993   critical for maintaining glucose homeostasis. *JCI Insight* **5**.
994

995 **Figure legends**

996 **Figure 1.** Pancreas dissociation and FACS purification of islet cells from fetal and neonatal pigs.

997 (A) Schematic representation of the study design. (B) qRT-PCR analysis of *INS*, *GCG*, *SST*,

998 *KRT*, and *AMY2* of FACS sorted β-, α- and δ-cell populations from P22 neonatal pigs. The fold

999 change ($2^{-\Delta\Delta CT}$) relative to the unsorted cell population is shown on the y-axis. (C) Heatmap

1000 of differentially expressed genes (DEGs) in pig β-cells between early fetal, late fetal and

1001 neonatal stages. (D) GO Term enrichment analysis of genes increasing with age in pig β-cells.

1002 (E) Heatmap of DEGs in pig α-cells between early fetal, late fetal and neonatal stages. (F) GO

1003 Term enrichment analysis of genes increasing with age in pig α-cells. (G) Heatmap of DEGs in

1004 pig δ-cells between late fetal and neonatal stages. (H) GO Term enrichment analysis of genes

1005 increasing with age in pig δ-cells. The Z-score scale represents $\log_2(X+1)$ transformed

1006 transcripts per million (TPM) counts. Red and blue color intensity of the Z-score indicates up-

1007 regulation and down-regulation, respectively. Adjusted *P* value threshold for GO term analysis

1008 was 0.1.

1009

1010 **Figure 2.** Analysis of gene expression in developing pig islet β-, α- and δ-cells. (A-E,G,H)

1011 Boxplots displaying normalized TPM (transcripts per million) counts of β-, α-, and δ-cell specific

1012 genes (A-D), markers associated with proliferation (E), disallowed genes (G) and β-cell

1013 functional regulators (G). (F) Quantification showing average percentage of INS$^+$, GCG$^+$ or SST$^+$

1014 cells that are Ki67$^+$ in each developmental stage (n = 40 images per group, from 3 pigs per

1015 group; bars show SD). Adjusted *P* value * *P≤0.05; ** P≤0.01; *** P≤0.001*

1016

1017 **Figure 3.** Stage-specific expression of islet factors during development. (A-C) Immunostaining

1018 of INS (green) and GCG (white) paired with Somatostatin (SST; red) (A), E-Cadherin (ECad;

1019 white) (B), and Chromogranin-A (CHGA; white) (C) in the early fetal, neonatal, and adult pig

1020 pancreas. (D-F) Immunostaining of the transcription factors PDX1 (D), NKX6.1 (E), and MAFB

1021 (F) in the early fetal, neonatal, and adult pig pancreas. (**G**) Immunostaining of SIX3 with INS and

1022 GCG in adult pig pancreas. Insets indicated by the dashed yellow box. Scale bars, 50 μm. (**H, I**)

1023 qRT-PCR measures of relative mRNA levels encoding *SIX3* (**H**) and *SIX2* (**I**) in isolated

1024 neonatal and adult pig islets (n=2, t-test; Error bars indicate SD). ΔCT values for neonatal and

1025 adult *SIX3* expression were 5.1 and 2.0, respectively (compared to β–Actin). ΔCT values for

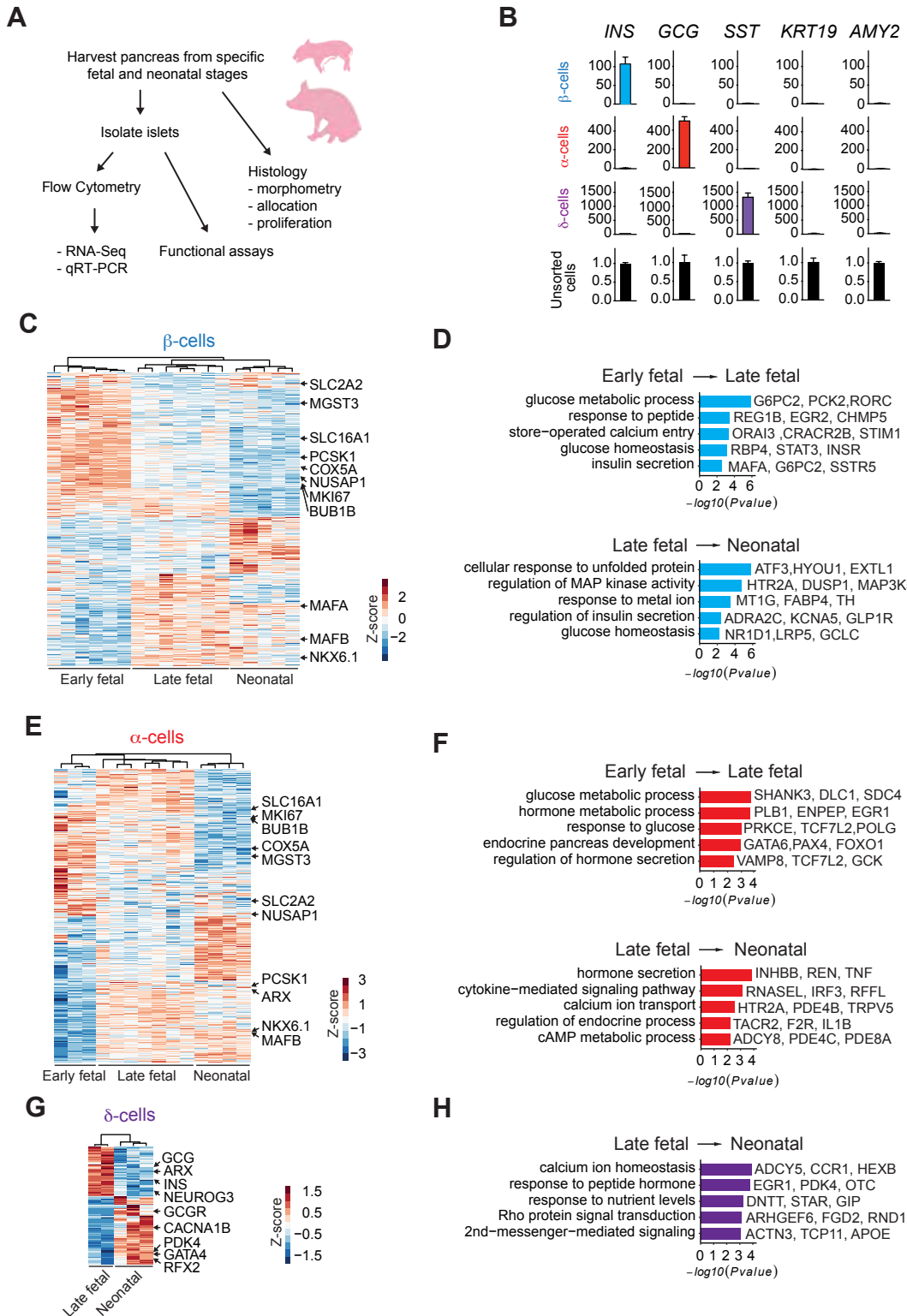1026 neonatal and adult *SIX2* (compared to β–Actin) were 7.2 and 2.6, respectively.

1027

30

1028   **Figure 4.** Comparison of gene expression in pig and human β- and α-cell development. (A)

1029   Unsupervised hierarchical clustering using distance matrices of neonatal pig, human, and

1030   mouse β-cells. (B-G) Boxplots displaying normalized TPM (transcripts per million) counts of

1031   select genes whose expression changes in a conserved manner between human and pig

1032   development. Adjusted *P* value * *P≤0.05; ** P≤0.01; *** P≤0.001.*

1033

1034   **Figure 5.** Dynamic gene regulation during pig β- and α-cell development. (A-B) Heat maps of

1035   genes with altered expression from early fetal to neonatal stages in β-cells (A) and α-cells (B),

1036   showing 8 distinct clusters. Cluster 2 includes genes whose mRNA increased up to late fetal

1037   stages then did not change thereafter. Cluster 7 includes genes whose mRNA declined then did

1038   not change thereafter. Enriched GO terms in each cluster are shown to the right. Adjusted *P*

1039   value threshold was 0.1. The Z-score scale represents $\log_2(X+1)$ transformed transcripts per

1040   million (TPM) counts. Red and blue color intensity of the Z-score indicates up-regulation and

1041   down-regulation, respectively. (C-D) The Z-score scale represents $\log_2(X+1)$ transformed TPM

1042   counts with total genes in β-cells (C) and α-cells (D). Cluster 3 (Up-Down) or Cluster 6

1043   (Down_Up). Boxplots displaying normalized TPM (transcripts per million) counts of genes

1044   shown. (E) Boxplots displaying normalized TPM (transcripts per million) counts of PCSK1

1045   mRNA. (F) Immunostaining of PCSK1 (white) with insulin (INS; green) and glucagon (GCG; red)

1046   in early fetal, late fetal and adult pig pancreas. Insets indicated by the dashed yellow box. White

1047   arrows indicate PCSK1^{+} GCG[+] (double positive) cells. (G) Concentrations of active GLP-1 in

1048   lysates from pig islet cell clusters at different developmental stages (ANOVA, ** *P≤0.01*; bars

1049   indicate SD). (H) Boxplots displaying normalized TPM (transcripts per million) counts of *DPP4*

1050   mRNA. (I) Immunostaining of DPP4 (white) with insulin (INS; green) and glucagon (GCG; red) in

1051   early fetal, neonatal and adult pig pancreas. Insets indicated by the dashed yellow box. White

1052   arrows indicate DPP4^{+} INS[+] (double positive) cells. Adjusted *P* value * *P≤0.05; ** P≤0.01; ****

1053   *P≤0.001*, Scale bars, 50 µm.

1054

1055   **Figure 6.** Maturation of β-cell function in postnatal pigs. (A) Glucose-stimulated insulin secretion

1056   (GSIS) assay measured insulin secretion in response to 2.8mM (low), 20mM (high) glucose and

1057   20mM glucose + IBMX. Data show average secreted insulin as a percentage of insulin content

1058   in the isolated islets from late fetal (n=4) and P22 (n=3) piglets (t-test, ** *P≤0.01; *** P≤0.001*;

1059   bars indicate SD). (B) Heat map of DEGs between late fetal and P22 β-cells. The Z-score scale

1060   represents $\log_2(X+1)$ transformed transcripts per million (TPM) counts. Red and blue color

1061   intensity of the Z-score indicates up-regulation and down-regulation, respectively. (C,E) GO

31

1062   term analysis for biological processes with up-regulated (C) and down-regulated (E) genes

1063   between late fetal and P22 β-cells. Adjusted *P* value threshold was 0.1. (D,F) Boxplots

1064   displaying normalized TPM (transcripts per million) counts of up-regulated (D) or down-

1065   regulated (F) genes between late fetal and P22. Adjusted *P* value * *P≤0.05; ** P≤0.01; ***

1066   *P≤0.001.*

Fig. 1

Fig. 2

Fig. 3

Fig. 4

Fig. 5

A

% Secretion (Condition / total content)

Legend:
- 2.8mM Glucose
- 20mM Glucose
- 20mM Glucose +IBMX

Late fetal: N.S
P22: ***, **

B

Z-score: 2, 1, 0, -1, -2

Gene labels (top to bottom): KCNQ1, PPARGC1A, CRACR2A, PDE7B, CAMK2D, CACNB4, SLC2A2, HCN4, ACTN2, GLP1R, GPR68, ENO2, ADRA2A, GCK, GPD1, STX1B, SYT2, ALDOB

Late fetal | P22

C

Up regulated

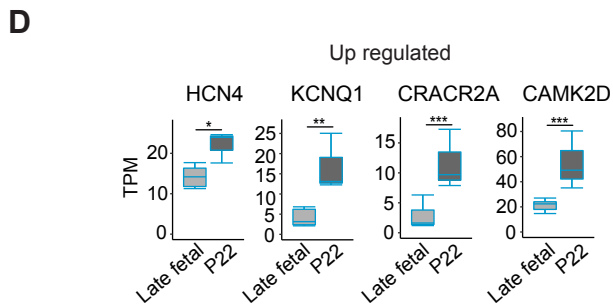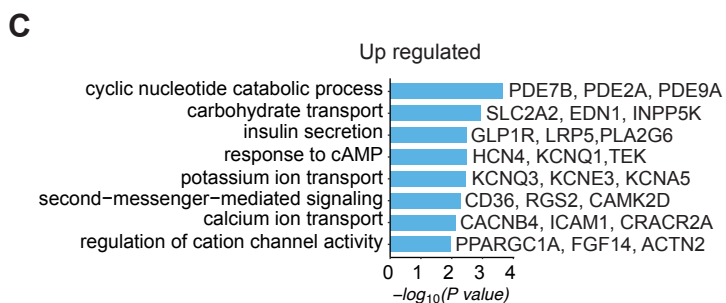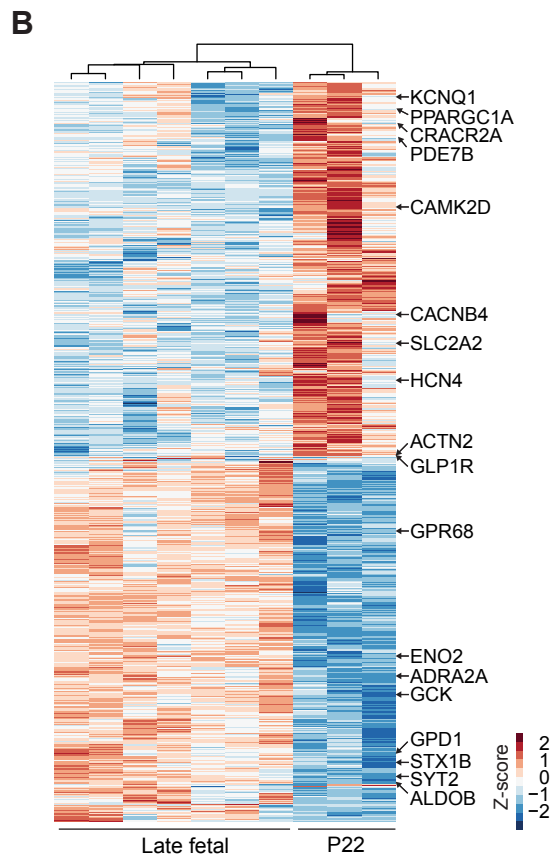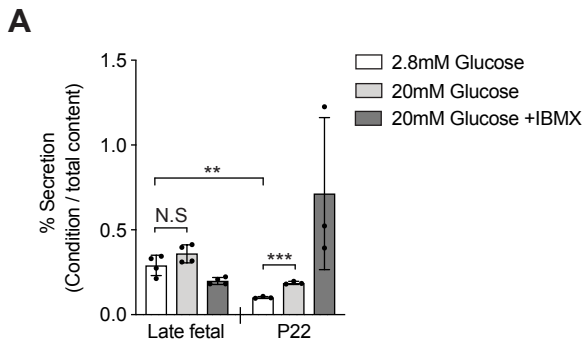| Term	Genes
cyclic nucleotide catabolic process	PDE7B, PDE2A, PDE9A
carbohydrate transport	SLC2A2, EDN1, INPP5K
insulin secretion	GLP1R, LRP5, PLA2G6
response to cAMP	HCN4, KCNQ1, TEK
potassium ion transport	KCNQ3, KCNE3, KCNA5
second−messenger−mediated signaling	CD36, RGS2, CAMK2D
calcium ion transport	CACNB4, ICAM1, CRACR2A
regulation of cation channel activity	PPARGC1A, FGF14, ACTN2

$-log_{10}(P\ value)$

D

Up regulated

TPM

HCN4 (*), KCNQ1 (**), CRACR2A (***), CAMK2D (***)

Late fetal | P22

E

Down regulated

Term	Genes
glucose catabolic process	PFKM, GAPDH, GCK
response to glucose	ACVR1C, EPHA5, GPR68
protein S/T kinase signaling pathway	CITED1, CDKN1C, BMP3
calcium ion regulated exocytosis	SCIN, SYT2, STX1B
ATP generation from ADP	CBFA2T3, GPD1, GCKR

$-log10(Pvalue)$

F

Down regulated

TPM

ENO2 (*), ALDOB (***), GPD1 (***), GCK (*)

Late fetal | P22

Fig. 6